Rahman, M.M.; Lillepaerg, J.; Neumann, S.; Shishatskiy, S.; Abetz, V.:

A thermodynamic study of CO2 sorption and thermal transition of PolyActive™ under elevated pressure

In: Polymer (2016) Elsevier

DOI: 10.1016/j.polymer.2016.04.024

A thermodynamic study of CO_2 sorption and thermal transition of PolyActive™ under elevated pressure

Md. Mushfequr Rahman[a], Jelena Lillepärg[a], Silvio Neumann[a], Sergey Shishatskiy[a], Volker Abetz[a,b]*

[a]Helmholtz-Zentrum Geesthacht, Institute of Polymer Research, Max-Planck-Straße 1, 21502 Geesthacht, Germany

[b]University of Hamburg, Institute of Physical Chemistry, Grindelallee 117, 20146 Hamburg, Germany

*Corresponding Author. Email: volker.abetz@hzg.de

Abstract:

The sorption of CO_2 in two commercial grades of multiblock copolymers (PolyActive™) is investigated using a magnetic suspension balance in the temperature range 30 – 70 °C. The isotherms follow Henry's law when the poly(ethylene glycol) (PEG) blocks of PolyActive™ are in a molten state. A significant deviation is observed when the PEG blocks are still in a semicrystalline state. Differential scanning calorimetry (DSC) is used to study the thermal transitions of the polymers. The melting and crystallization of the PEG blocks is studied using high pressure differential scanning calorimetry in both CO_2 and N_2 gas environment. A substantial decrease of melting and crystallization temperature occurs with increasing CO_2 pressure. But no change occurs under N_2 pressure. The observed experimental results are discussed on the basis of established thermodynamic equations reported in the literature which provide an adequate guideline to correlate the sorption isotherms with the thermal transition of the PEG blocks.

Key Words: PolyActive™, CO_2 sorption, Melting point depression, High pressure differential scanning calorimetry, Semicrystalline polymer.

1. Introduction:

Semicrystalline polymers, endowed with the coexistence of amorphous and crystalline phases, constitute a large group of commercially available polymeric materials. The degree of crystallinity and the crystalline morphology are two of the most salient features that dictate the final properties of these polymers. It is already well-known that the interaction of a compressed gas (e.g. CO_2) with a semicrystalline polymer can bring about depression of both glass transition temperature and melting temperature.[1] Depending on the application and process conditions this phenomenon can be either beneficial or troublesome. In either case a quantitative knowledge of melting point and crystallinity of the polymer as a function of process conditions is of utmost importance for several application such as – foam fabrication, packaging materials production, membrane based gas separation, high pressure polymerization etc.[2] In presence of a compressed gas a semicrystalline polymer may attain a substantially different crystalline morphology compared to what is obtained at ambient condition.[1] In this regard researchers have extensively investigated the CO_2 induced crystallization and melting of various polymers, e.g. polypropylene[3, 4], syndiotactic polystyrene[1, 5], poly(ethyelene terephthalate)[1, 6-9], polycarbonate[10], polycaprolactone[11-13], poly(ether ether ketone)[14, 15], poly(phenylene sulfide)[16], poly(3-hydroxybutyrate-*co*-3-hydroxyvalerate)[17], pluronics[18] etc.

A fundamental understanding of polar and nonpolar gas solubility in semicrystalline poly(ethylene glycol) (PEG) is essential to provide incentives for development of both gas-transport[19] and gas-barrier[20] materials. The polar ether oxygen has strong affinity for the acidic CO_2 gas due to the polar-quadrapolar interaction.[21] This phenomenon is extensively exploited to design gas separation membrane through which CO_2 permeates faster than the non-polar gases such as N_2, H_2, CH_4 etc. It is generally accepted that in the crystalline phase the polymer chain packing is too dense to leave voids suitable for penetration of even the small gas molecules. On the other hand the amorphous phase having randomly arranged and highly mobile polymer segments offers ample free volume for gas permeation. [19, 20] Hence for the gas separation membranes (working according to the solution-diffusion mechanism) it is crucial to ensure that PEG is in an amorphous state under operating conditions. Block copolymers (e.g. PEBAX®, PolyActive™) containing alternating series of short PEG block and a semi-crystalline block froming the hard phase exhibit superior gas separation performance compared to PEG homopolymer. In these block copolymers the presence of a crystalline block between individual PEG blocks inhibits the chain packing efficiency of the polar ether linkages. The crystallinity of the PEG blocks of these polymers depends on the length and content of the two different sorts of blocks.[22-26] We have used differential scanning calorimetry (DSC) to study the thermal transitions of the different blocks of the aforementioned multi-block copolymers. The method provides appreciable assistance to correlate the sorption and diffusion of gases with other physical properties of the polymers.[25, 27, 28] High pressure DSC is a powerful tool which allows us to study the *in-situ* thermal transitions in presence of CO_2 or other gases at high pressure. It gives us the opportunity to understand the interaction of polymer and gas molecule

during glass transition, melting, crystallization etc.[6] In this work we aim to provide an insight into the thermodynamic behavior of CO_2 sorption in the commercial thermoplastic elastomer PolyActive™ at different pressures. In this regard we use high pressure DSC and magnetic suspension balance to construct a robust correlation between gas sorption and phase transformation of the PEG block of PolyActive™ at different temperatures and pressures. Two grades of PolyActive™ are used for this study which have the commercial names PolyActive™3000PEGT77PBT23 and PolyActive™4000PEGT77PBT23. For both of these polymers the weight percentage ratio of the two types of blocks namely poly(ethylene glycol terephthalate) (PEGT) and poly(butylene terephthalate) (PBT) are 77wt% and 23 wt%, respectively. For discussion in this manuscript we address them as P 3000 and P 4000, respectively, which represents the molecular weight in g/mol of the PEG segment in the PEGT block.[25]

2. Experimental:

2.1. Materials:

Both grades of the PolyActive™ were purchased from PolyVation, The Netherlands and chloroform (purity 99.0–99.4%) was purchased from Merck, Germany. The chemicals were used as received without any further purification. Nitrogen (purity 99.999%) was supplied by Air Liquide, Germany and carbon dioxide (purity 99.995%) was supplied by Linde, Germany.

2.2. Thick film casting:

3 wt% solutions of P 3000 and P 4000 were prepared using chloroform as solvent. The obtained homogeneous solutions were poured in Teflon® molds. The molds were covered with glass Petri dish to ensure slow evaporation of solvent and kept at room temperature for film formation.

2.3. Characterization:

2.3.1. Gas sorption measurement:

The sorption measurements of pure CO_2 were performed with a gravimetric sorption analyzer IsoSORP® Static from Rubotherm (Bochum, Germany). The detailed description of the instrument and technique was given elsewhere.[29, 30] The IsoSORP® system is equipped with a precision pressure sensor DPI 282 with an accuracy of ±0.006 bar. The experimental temperature was maintained with the cryo-compact circulator (temperature stability ±0.03 °C) from Julabo GmbH, Germany. Adsorption isotherms of CO_2 were determined in the temperature range 30 – 70 °C at each 10 °C and pressure ranging from zero to 30 bar with a resolution and a reproducibility of the Magnetic Suspension Balance (MSB) (Rubotherm, Germany) of 0.01 mg and ± 0.03 mg, respectively. The additional option of the IsoSORP® instrument allowed us to take into account the gas nonideality through the weighing *in-situ* of an inert sample. Prepared

films of P 3000 and P 4000 with thickness of 200-260 µm were evacuated *in-situ* overnight at 80 °C to remove gases and residual volatile compounds dissolved in the polymer matrix before the measurement. The specific uptake was determined as described elsewhere[31] taking into account buoyancy in gas. Furthermore, the density measurement was performed by Archimedes' principle using the standard equipment for Excellence Plus Mettler Toledo, Germany analytical balances. The FLUORINERT^{TM} FC-77 from 3M, USA was used as auxiliary liquid in order to prevent liquids adsorption on the PolyActive^{TM}. To take into account the real gas behavior of CO_2 the gas fugacity was determined from the Soave-Redlich-Kwong equation of state[32] using the chemical process optimization software Aspen Plus®.

2.3.2. Differential scanning calorimetry study:

To study the thermal transition of the prepared films under a N_2 purge gas stream a DSC 1 (Star system) from Mettler Toledo, Germany was used. At first the samples were heated up to 100 °C, kept at this temperature for 5 min to erase any effects resulting from sample preparation. Then the sample was cooled down to −100 °C and a second heating scan up to 250 °C followed by the cooling scan down to −100 °C were performed. The DSC runs were performed at a scan rate of 10 K/min. A High Pressure DSC 1 from Mettler Toledo was used to study the *in-situ* thermal transition of PolyActive^{TM} 4000PEGT77PBT23 at elevated pressure. The temperature protocols are described in section 3.3.

3. Results:

3.1. Gas sorption measurement:

The density of P 3000 and P 4000 determined in N_2 atmosphere using MSB at 30 °C is in good agreement with that obtained by Archimedes method using FLUORINERT^{TM} FC-77 liquid at 23.5 °C (Figure S 1 and S 2). Elevation of temperature causes a small decrease of density. The change in density is taken into account for determination of specific uptake of CO_2 by the polymers in the temperature range 30 – 70 °C. The isotherms of specific CO_2 uptake with respect to fugacity of CO_2 are plotted in Figure 1. At 30 °C the specific CO_2 uptake vs fugacity curve has a curvature convex to the fugacity axis for both polymers. Up to 10 bar both polymers show similar CO_2 uptake. For higher fugacity the increase in specific uptake increases dramatically in P 3000 compared to P 4000. At 40 °C the CO_2 uptake is higher in P 3000 compared to P 4000. P 3000 shows almost linear increase of CO_2 uptake with increasing fugacity. P 4000 shows this phenomenon up to 20 bar CO_2 fugacity. The CO_2 uptake of P 4000 increases dramatically when the fugacity exceeds 20 bar and becomes very close to the CO_2 uptake of P 3000 at 30 bar. It can be clearly seen that the specific CO_2 uptake vs fugacity curve of P 4000 at 40 °C is analogous to that of P 3000 at 30 °C. Between 50 °C to 70 °C specific CO_2 uptake for both P 3000 and P 4000 increases linearly with increasing fugacity. Both of the polymers have the same value of CO_2 uptake which decreases with increasing temperature. It is worth mentioning that when CO_2

uptake is plotted against fugacity (Figure 1) instead of pressure (Figure S3) a small deviation from linear increase is observed. For example a plot of CO_2 uptake (in mol/g) of P4000 at 50 °C using both ideal (i.e. compressibility factor of CO_2, $Z_{CO_2} = 1$) and real ($Z_{CO_2} < 1$) gas behavior is provided in the supporting information (Figure S 4). The Henry's law constant, k_H is calculated from the slope of such plots (Table 1). Table 1 shows that the value of k_H differs significantly for $Z_{CO_2} = 1$ and $Z_{CO_2} < 1$. The official definition of k_H provided by the IUPAC contains fugacity instead of pressure.[33] For any practical calculation the values of k_H obtained by considering $Z_{CO_2} < 1$ are most appropriate. The temperature dependence of k_H can be described by the following equation:

$$\frac{-d \ln k_H}{d\left(\frac{1}{T}\right)} = \frac{\Delta H_S}{R} \qquad (1)$$

where T is absolute temperature [K], ΔH_s is the molar heat of dissolution [kJ mol^{-1}]and R is the gas constant [kJ K^{-1} mol^{-1}]. ΔH_s of CO_2 dissolution in P 3000 and P 4000 is calculated according to equation 1 from the slope of *ln* k_H vs *1/T* plot (Figure S 5).[34] Similar to k_H the obtained value of ΔH_s (Table 1) is also slightly different for $Z_{CO_2} = 1$ and $Z_{CO_2} < 1$. ΔH_s has a negative value which implies that CO_2 dissolution in P 3000 and P 4000 is an exothermic process (discussed in detail in section 4.1).

3.2. Differential scanning calorimetry:

Figure 2 shows the second heating and second cooling trace for the two polymers under study. Two distinct melting endotherms and crystallization exotherms are observed which is consistent with the phase separated morphology of the polymers. The onset, peak and endset temperatures of the transitions are tabulated in supplementary information (Table S 6). The melting endotherm of the PEG block of P 3000 starts at 32 °C and ends at 45 °C (Figure 2a). The onset and endset of the melting endotherm of PEG blocks of P 4000 are 40 °C and 50 °C, respectively (Figure 2a). The PBT blocks show a broad melting endotherm between 105 °C to 205 °C for both polymers (Figure 2b). The exact peak temperature of such broad transition deviates a lot. The crystallization of PBT block of P 3000 and P 4000 starts at 160 °C and 170 °C, respectively, (Figure2b) upon cooling from the melt. As the temperature is decreased further, crystallization of the PEG blocks takes place. For P 3000 it starts at 23 °C and ends at 18 °C (Figure 2a). The crystallization exotherm of the PEG blocks of P 4000 has an onset and endset of 30 °C and 25 °C (Figure 2a). The crystallinity of PEG blocks calculated from the analysis of the DSC curves (considering 166 Jg^{-1} as heat of fusion of a 100% crystalline PEG [35]) is 54% and 57% for P 3000 and P 4000, respectively.[25] Hence for both polymers the length of PEG blocks does not have a big influence on the crystallinity of PEG blocks, but both melting and crystallization takes place at a higher temperature for P 4000 compared to P 3000. This difference in melting and crystallization temperatures of the polymers is responsible for the different CO_2 uptake at 30 °C and 40 °C (discussed in detail in section 4.1).

3.3. High pressure differential scanning calorimetry:

In this section we report the melting and crystallization of the PEG block of P 4000 induced by pressurized CO_2 and N_2 studied using a high pressure DSC. It is not possible to study the thermal transition of the PBT blocks as the sample degrades in a pressurized CO_2 atmosphere when heated up to 200 °C (Figure S 7). The influence of CO_2 saturation at a pressure up to 35 bar on melting and crystallization of PEG block of P 4000 is depicted in Figure 3. Two different temperature protocols are used for the study. For one set of experiments the samples were first heated up to 220 °C at 10 K/min to erase the thermal history. Then they were allowed to cool down at 70 °C. The cooling rate of this step was not controlled. At this point the crystallization of PBT block is finished, yet the PEG block remains in a molten state. The samples were pressurized with CO_2 for 1 hour at 70 °C. Then the samples were scanned down to 20 °C and subsequently up to 70 °C at 0.5 K/min without releasing the CO_2 pressure. However, as expected change of temperature at constant volume has an influence on pressure as well. This temperature protocol allows us to study the influence of CO_2 pressure on crystallization of PEG block while cooling down from the melt (Figure 3b) and the subsequent melting (Figure 3c) in a confinement imposed by the already crystallized PBT block. The saturation time is varied from 15 min to 4 h to investigate the change in crystallization temperature at 15 bar CO_2 pressure (Figure S 8). Since no change is observed, we use 1 h saturation time for all the experiments. Figure 3b and 3c show the cooling and heating traces followed by the CO_2 saturation at 70 °C. At 1 bar CO_2 saturation pressure the PEG block crystallization starts at 35 °C. The crystallization temperature and the area of crystallization exotherm decrease significantly with the increase of CO_2 pressure. At 35 bar the onset of crystallization is 27 °C. In other words, for the crystallization to start at 35 bar CO_2 pressure the temperature has to be 8 °C lower compared to that at 1 bar CO_2 pressure. The subsequent heating cycle shows that the melting endotherm also shifts to a lower temperature. Moreover, a substantial decrease of the area of crystallization exotherm and melting endotherm occurs with the increase of CO_2 pressure.

Another set of experiments were performed using the temperature protocol depicted in Figure 3d. At first the thermal history was erased by sample heating up to 220 °C and the PBT blocks were allowed to crystallize by cooling down to 70 °C. In contrast to the other temperature protocol (Figure 3a) in this case the samples were cooled down to 20 °C at 0.5 K/min rate to make sure crystallization of the PEG blocks is complete and then pressurized with CO_2. Therefore the PEG blocks were already in a semicrystalline state when the sample was saturated with CO_2 and the following heating cycle shows the influence of CO_2 saturation pressure on the melting of an already crystallized PEG block. The heating trace (Figure 3f) shows that depression of the melting point of PEG blocks occurs with increasing pressure. The area of the peak under the melting endotherm also decreases with increasing CO_2 pressure. It is important to mention that the shape of melting peaks obtained from two temperature protocols is significantly different. The shape of the melting peaks suggest that when CO_2 pressure is applied upon semicrystalline PEG at 20 °C a part of the crystals dissolve which leads to two populations of differently sized

PEG crystals. The onset and endset temperatures of the crystallization exotherms depicted in Figure 3b and 3e are plotted against the pressure in Figure 4 for comparison. It is evident that for saturation at 70 ºC the onset and endset temperatures are lower compared to those obtained after saturation at 20 ºC. A significant increase of the width of crystallization exotherms obtained from both temperature protocols is observed with increasing CO_2 pressure.

However, there is no influence of N_2 saturation (at 70 °C) on the crystallization exotherms (Figure 5b) and melting endotherms (Figure 5c) of the PEG block of P 4000. It is noteworthy that the crystallization temperatures (onset, peak and endset) of the PEG block of P 4000 obtained from high pressure DSC (High Pressure DSC 1 from Mettler Toledo) at a scan rate of 0.5 K/min under 1 bar CO_2 (Figure 3b) and 1 bar N_2 (Figure 5b) are analogous. However, the onsets of these crystallization exotherms are approximately 5 °C higher than that depicted in Figure 2a which was obtained using a different device (DSC 1 (Star system) from Mettler Toledo) under a N_2 purge gas stream at 10 K/min. Therefore the thermal transitions of PEG block of P 4000 was studied in DSC 1 (Star system) using the temperature protocol depicted in Figures 3a and 5a with N_2 as a purge gas stream. The peak temperatures of crystallization and melting of the PEG block of P 4000 in CO_2 and N_2 atmospheres using the temperature protocol depicted in Figure 3a and 5a, respectively, (i.e. the same temperature protocol) are plotted against applied gas pressure in Figure 6. It is evident that irrespective of the device and gas (i.e. N_2 or CO_2) at 1 bar pressure the melting and crystallization temperatures are analogous while those decrease linearly with increasing CO_2 pressure and remain unchanged with the increasing N_2 pressure. Therefore the deviation of crystallization temperature observed in Figure 2a originates from the faster scan rate (i.e 10 K/min instead of 0.5K/min) used for the DSC run.

4. Discussion:

4.1. Thermodynamics of CO_2 sorption:

The sorption of a gas in a rubbery polymer is generally accepted to be described using Henry's law:

$$C = k_H P \qquad (2)$$

where C is the concentration of gas in the polymer, P is the gas pressure and k_H is the Henry's law constant.[36] The solubility coefficient, S can be expressed as follows:

$$S = \frac{C}{P} \qquad (3)$$

Thus when there is no concentration dependence S and k_H are equal.[37] According to equation 2 the specific gas uptake of a rubbery polymer should increase linearly with gas pressure. The

specific CO_2 uptake of P 3000 and P 4000 follows equation 2 in the temperature range 50 - 70 °C (Figure 1). In this temperature range the specific CO_2 uptake also decreases with increasing temperature. The temperature dependence of the solubility is given by the following equation:

$$S = S_0 \exp\left(\frac{-\Delta H_S}{RT}\right) \qquad (4)$$

where S_0 is the pre-exponential factor (solubility at infinitely high temperature), ΔH_s is the molar heat of sorption, R is the gas constant and T is temperature in Kelvin. The large negative value of ΔH_s (table 1) implies that the dissolution of CO_2 in both P 3000 and P 4000 is an exothermic process which in turn causes the decrease of specific CO_2 uptake with increasing temperature. A combination of two thermodynamic processes is involved in the dissolution of a gas molecule in a polymer matrix – 1) condensation of the gas molecule at the surface 2) formation of a molecular scale gap in the polymer to accommodate the gas molecule. Therefore ΔH_s can be written as:

$$\Delta H_S = \Delta H_{condensation} + \Delta H_{mixing} \qquad (5)$$

where $\Delta H_{condensation}$, the molar heat of condensation and ΔH_{mixing}, the partial molar heat of mixing are the enthalpies of changes for the first and second thermodynamic process, respectively. $\Delta H_{condensation}$ is always a negative term and ΔH_{mixing} is usually positive.[36-38] The critical temperature and pressure of CO_2 is 31.04 °C and 73.8 bar, respectively. So in the temperature and pressure range where CO_2 dissolution is studied the value of ΔH_S depends predominantly on $\Delta H_{condensation}$. As the temperature increases CO_2 has more and more difficulty to condense in the polymer which causes the decrease of specific CO_2 uptake.[37] It gives a satisfactory account for the specific CO_2 uptake of P 3000 and P 4000 between 50 – 70 °C (Section 3.1, Figure 1) where the PEG blocks are in a completely molten state.

The isotherm of P4000 is convex to the fugacity axis at 30 and 40 °C while P3000 shows such isotherm only at 30 °C. In a rubbery polymer e.g. polydimethylsiloxane this convex curvature is attributed to the swelling of polymer due to sorption of the gas.[39] In absence of strong polymer-penetrant interaction such sorption behavior can be described from the classical theory of Flory and Huggins using the following equation:

$$\ln\left(\frac{f}{f_0}\right) = \ln \phi_g + \left(1-\phi_g\right) + \chi\left(1-\phi_g\right)^2 \qquad (6)$$

where f is the gas fugacity, f_0 is the standard state fugacity of the gas, ϕ_g is the volume fraction of the gas in polymer and χ is the polymer-gas interaction parameter.[40] But both P 3000 and P 4000 exhibit the convex curvature only at a temperature where the PEG blocks exist in a semicrystalline state (discussed in section 3.2). If the curvature of the isotherms was due to the swelling of the amorphous part of P 3000 and P 4000 it would not disappear at a temperature

higher than the melting of the PEG block. It is evident that the curvature appears due to the influence of CO_2 pressure upon the crystalline PEG part of the polymers. Michaels et al. studied the solubility of several gases (including CO_2 and N_2) in a semicrystalline polyethylene. They proposed a two phase model composed of distinct amorphous and crystalline phases where the crystals are dispersed in an amorphous matrix and act as a nonsorbing and impermeable phase. They found that the solubility constant is proportional to the volume fraction of amorphous phase in polyethylene i.e.

$$S = \alpha S^* \qquad (7)$$

where α is the volume fraction of amorphous phase and S^* is the solubility constant in a hypothetical completely amorphous polyethylene.[19, 41-43] If we consider equation 7 for solubility of P 3000 and P 4000 between 30 – 70 °C it is obvious that the value of α increases until the PEG block is in a completely molten state. The melting of PBT takes place above 100 °C (Section 3.2, Figure 2). Therefore in the temperature range where CO_2 sorption is studied (30 – 70 °C) the PBT block is in a semicrystalline state. Up to the point where melting of the crystals of the PEG blocks is complete the increase of temperature leads to a higher amorphous PEG phase content which tends to increase the CO_2 solubility. Meanwhile, the negative value of ΔH_S tends to decrease the CO_2 solubility with increasing temperature. These two counteracting phenomenon explain the observed difference of specific CO_2 uptake in P 3000 and P 4000 at 30 and 40 °C. Since the melting of PEG blocks of P 4000 takes place at a higher temperature than that of P 3000 the amorphous PEG phase content is higher in the latter at any point below the melting temperature. For this reason at 40 °C a higher CO_2 uptake is observed in P 3000. Moreover, the melting point of P 4000 decreases with the increase of CO_2 pressure. As a result the value of α also increases when the CO_2 pressure is raised keeping the temperature constant at 30 and 40 °C. Due to this added amorphous phase content at elevated pressure P 4000 dissolves more CO_2 then expected by Henry's law and the isotherms have a curvature convex to the fugacity axis. As at 40 °C most, if not all, of the PEG of P 3000 already exists in a molten state, this polymer has a curvature in the isotherm only at 30 °C. In what follows we discuss the thermodynamics behind the CO_2 induced melting point depression of the PEG blocks.

4.2. Thermodynamics of CO_2 induced melting:

"The equilibrium melting temperature of a polymer may be defined as the melting point of an assembly of crystals, each of which is so large that size (i.e. surface) effects are negligible, with the provision that each such large crystal is in equilibrium with the normal polymer liquid." – John J. Hoffman and James J. Weeks.[44]

At the equilibrium melting temperature the chemical potential of the polymer repeating unit of two phases (i.e. the molten and crystalline phase) are equal. The addition of a miscible diluent causes a decrease of the chemical potential of the repeating unit in the melt. As a result melting point depression occurs to meet the condition of equilibrium.[45] Paul J. Flory derived a

relationship of the equilibrium melting point of a polymer-diluent mixture, T_m to its composition. It can be stated as:

$$\frac{1}{T_m} - \frac{1}{T_m^0} = \frac{R}{\Delta H_u} \cdot \frac{V_2}{V_1} \left(\phi_1 - \chi \phi_1^2 \right) \qquad (8)$$

where, T^0_m is the equilibrium melting point of the pure polymer, ΔH_u is the heat of fusion per mole repeating unit, V_2 is the molar volume of polymer repeating unit, V_1 is the molar volume of the diluent, ϕ_1 is the volume fraction of the diluent and χ is the polymer-diluent interaction parameter. The depression of the melting point by the diluent is approximately proportional to the term $1/T_m - 1/T^0_m$.[45] From section 3.3 it is evident that in the presence of pressurized CO_2 the PEG segments of P 4000 tend to retain the disordered state instead of folding and aligning with each other to form crystals. In the absence of a diluent the crystalline state of a polymer has lower free energy compared to its molten state when the temperature is below melting. Therefore the value of $\chi_{PEG\text{-}CO_2}$ i.e. the interaction parameter of the PEG block of P 4000 with CO_2 is low enough to diminish the thermodynamic driving force of the polymer to exist in a crystalline state which results in the decrease of crystallization and melting points. But no change of the melting behavior is observed when DSC scans are performed in N_2 atmosphere (pressure range 1-25 bar) instead of CO_2. This is an obvious manifestation of the fact that the quadrapolar CO_2, due the high affinity towards polar ether oxygens, has a much stronger affinity towards the PEG block of P 4000 compared to that of nonpolar N_2. Hence, $\chi_{PEG\text{-}CO_2} << \chi_{PEG\text{-}N_2}$ where, $\chi_{PEG\text{-}N_2}$ is the interaction parameter of polyether block of P 4000 with N_2. Moreover, the extent of depression of melting point increases with the CO_2 saturation pressure which means the melting temperature is influenced by ϕ_1. Thus equation 8 is qualitatively valid for the CO_2 induced depression of melting point of the PEG blocks of the multiblock copolymers under study. However, equation 8 represents the dependence of the depression of the melting point on the composition of the polymer-diluent mixture due to thermodynamic effects only.[45] In principal it will take infinitely long time for the formation of a perfect chain extended crystal which may undergo melting at equilibrium melting temperature. Polymer crystals formed within a limited time practically melt well below the equilibrium melting temperature due to their small size and imperfection. Even for the slowest scanning rate in our study, kinetic factors are involved for the experimentally observed thermal transition of a polymer together with the thermodynamic ones.[44, 46] Therefore, the CO_2 induced melting point depression of the PEG block of P 4000 in a high pressure DSC at a scan rate of 0.5 K/min (observed in Figure 3) occurs under the kinetic restraints which cannot be described by equation 8.

Zhang *et al.* [1] have studied the crystallization of poly(ethylene terephthalate) (PET) and syndiotactic poly(styrene) (PS) under pressurized N_2 and CO_2 using non-isothermal DSC scans of 5K/min. Similar to our observation they also found that the depression of melting point occurs under compressed CO_2 atmosphere but not under N_2 atmosphere. They used the Gibbs-Thomson

equation to explain the depression of melting point which takes into account the experimental melting point due to the finite sized crystals:

$$T_m^{'} = T_m^o\left(1-\frac{2\sigma}{l\Delta H_u}\right) \qquad (9)$$

where T'_m is the experimentally observed melting temperature of a crystallite of thickness l, T^o_m is the equilibrium melting point of a perfect crystal composed of infinitely long polymer chains, σ is the interfacial free energy associated with the basal plane of the lamellar crystallite and ΔH_u is the enthalpy of fusion per repeating unit of the polymer chain.[1, 46, 47] They observed that in the presence of compressed CO_2 the melting onset and the melting peak shifted to lower temperatures but the breadth of the peak was unchanged (which is not the case in our study). Thus considering T^o_m, l and ΔH_u as constant values they have concluded that gas is dissolved in the amorphous parts of the polymer and the depression of melting point occurs only due to the increase in σ caused by the dissolved CO_2. In contrast Figure 3 and 4 shows that the width and area of the melting endotherm and crystallization exotherm of the PEG blocks of P 4000 change substantially as the CO_2 pressure increases. Therefore, the postulations made by Zhang *et al.* [1] for PS-CO_2 and PET-CO_2 systems is not applicable for CO_2 induced melting and crystallization of PEG blocks of P 4000. The decrease of peak area implies the decrease of crystallinity with increasing CO_2 pressure which leads us to the conjecture that a part of the crystalline PEG is dissolved by CO_2 under elevated pressure. But it must be taken into account that during a DSC run under elevated CO_2 pressure, as the first crystals melt, the resulting molten phase becomes available for CO_2 dissolution. The resulting apparent endothermic peak can decrease due to this simultaneous exothermic effect. In other words the area under the melting peak is an overlap of endothermic heat of fusion and exothermic heat of dissolution.[48] This phenomenon creates considerable uncertainty to calculate the crystallinity from DSC traces depicted in Figure 3.

4.3. Correlation of CO_2 induced melting point depression with Henry's law constant:

The Gibbs-Thomson equation is originally derived considering only two phases (i.e. the molten and crystalline phase). An analog of the equation which takes into account the equilibrium between three phases (solid-liquid-vapor) to describe the melting of small crystallites is not yet developed.[46] When crystallization occurs from a molten state in presence of a compressed gas, it is rational to consider a two-component, three-phase system to describe the melting point behavior.[2] Such systems can be accurately described by the Clapeyron equation as it can be extended for n components and $n+1$ phase mixtures. For a two component, three phase solid-liquid-vapor equilibrium the equation is as follows –

$$\frac{dP}{dT} = \frac{\begin{vmatrix} \frac{1}{T}\sum x_i^V H_i^V & x_u^V & x_{CO_2}^V \\ \frac{1}{T}\sum x_i^L H_i^L & x_u^L & x_{CO_2}^L \\ \frac{1}{T}\sum x_i^S H_i^S & x_u^S & x_{CO_2}^S \end{vmatrix}}{\begin{vmatrix} V^V & x_u^V & x_{CO_2}^V \\ V^L & x_u^L & x_{CO_2}^L \\ V^S & x_u^S & x_{CO_2}^S \end{vmatrix}} \qquad (10)$$

where, x^j_i is the mole fraction of species *i* in phase *j*, V^j is the molar volume and H^j_i is the partial molar enthalpy. The phases rich in solid crystalline polymer, molten polymer and compressed gas are denoted by the subscripts S, L and V respectively.[2] When a polymer is exposed to a compressed gas two counteracting effects work simultaneously, namely solubility effect and pressure effect. The mutual interaction of polymer and gas tends to decrease the melting point (solubility effect) and the applied pressure tends to increase the melting point (pressure effect).[2] The linear decrease of melting point with increasing pressure suggests that in the studied pressure range the solubility effect outweighs the pressure effect. This is a typical behavior for a semicrystalline polymer exposed to an excess of sparingly soluble compressed gas. When the pressure is increased further a radical change is observed in the slope due to the dominating pressure effect. Weidner et al. reported this behavior for PEG with molar mass 4000 g/mol.[49] Lian *et al.*[2] have derived the following expression from equation 10 for the depression of melting point in the pressure range where solubility effect is dominant:

$$\frac{dT_m}{dP} \approx \frac{-T_m^2 R k_H}{\Delta H_u^{fusion}} \qquad (11)$$

where ΔH_u^{fusion} is the molar heat of fusion of the crystalline polymer. For the derivation of this equation Z=1 is considered for the compressed gas i.e. its deviation from ideal gas behavior at elevated pressure is neglected. Using the solubility data available in the literature authors have demonstrated that equation 11 can be used to calculate the k_H at the normal melting temperature. Figure 6 shows the comparison of k_H of P 4000 obtained from sorption balance with that calculated using equation 11 from the melting point depression observed in high pressure DSC. The endset of melting peak (in Kelvin) of the PEG blocks of P4000 obtained from Figure 3c and

3f are plotted against CO_2 saturation pressure (supporting information S 10). Since the values obtained from Figure 3c can more accurately described by a linear fit, the slope of this line i.e. -0.24 K/bar is used as the value of dT_m/dP. It must be noted that the k_H values obtained by sorption balance (plotted in Figure 6) are corrected for the amorphous phase content in the temperature range 50-70 °C to follow the procedure described by Lian *et al.*[2] From the DSC trace depicted in Figure 2 it is found that 57 wt% of the PEG content of P4000 is crystallizable. In the temperature range 50-70 °C only 6 wt% of P4000 exist in a crystalline state. The molten part (i.e. 94 % of the total weight of P4000) consists of the PEG block (ca. 82 wt%) and the non crystallizable part of the PBT block (ca. 18 wt.%). The theoretical value of meting enthalpy of a 100% crystalline PEG is 166 Jg^{-1} [35] while that of PBT is 140 Jg^{-1} [50]. According to these theoretical values the heat of fusion of a 100% crystalline polymer containing 82 wt% PEG and 18 wt% PBT is 161.32 Jg^{-1}. The k_H calculated considering the theoretical 100% crystalline polymer is labeled as "P4000_T_m" in Figure 7. It is clear that P4000_T_m is very close to the extrapolated line in the logarithmic plot when ideal gas behavior is assumed for CO_2 i.e. Z_{CO_2}=1. Therefore, equation 11 gives a pretty accurate estimation of the k_H of dissolution of gases in multiblock copolymers at the melting temperature when the heat of fusion of a 100% crystalline polymer is assigned as ΔH_u^{fusion}. It must also be noted that k_H obtained from equation 11 represents the quantity of gas absorbed per unit weight of the amorphous part of the polymer. For accurate estimation of k_H, the value has to be corrected for total weight of the polymer. The major limitation of equation 11 is it does not take into account the real gas behavior. There is a distinct difference between k_H values obtained by considering the ideal and real gas behavior of CO_2 as has been pointed out by Figure 7.

5. Conclusion:

From the presented results and subsequent discussion of this study it is evident that the CO_2 sorption isotherm of PolyActive™ is largely dictated by the thermal transition of the PEG blocks. The sorption isotherm show a significant deviation from Henry's law when the PEG blocks are in a semicrystalline state. This deviation occurs due to the CO_2 induced melting point depression of PEG blocks which stems from the strong affinity of the polar ether oxygen towards the quadrapolar CO_2. Equation 11 derived by Lian *et al.* [2] adequately correlates the Henry's law constant to the melting point depression of the PEG blocks of PolyActive™. But this relation is valid only at the melting temperature of PEG blocks. Future work should be directed towards developing a thermodynamic model which can predict the gas sorption behavior of a polymer-gas system having large affinity towards each other over a temperature range where the polymer exists in a semicrystalline state.

6. References:

[1] Z. Zhang, Y.P. Handa, CO_2-Assisted Melting of Semicrystalline Polymers, Macromolecules, 30 (1997) 8505-8507.
[2] Z. Lian, S.A. Epstein, C.W. Blenk, A.D. Shine, Carbon dioxide-induced melting point depression of biodegradable semicrystalline polymers, The Journal of Supercritical Fluids, 39 (2006) 107-117.
[3] J.-B. Bao, T. Liu, L. Zhao, G.-H. Hu, Carbon Dioxide Induced Crystallization for Toughening Polypropylene, Industrial & Engineering Chemistry Research, 50 (2011) 9632-9641.
[4] M. Takada, M. Tanigaki, M. Ohshima, Effects of CO_2 on crystallization kinetics of polypropylene, Polymer Engineering & Science, 41 (2001) 1938-1946.
[5] Y.P. Handa, Z. Zhang, B. Wong, Effect of Compressed CO2 on Phase Transitions and Polymorphism in Syndiotactic Polystyrene, Macromolecules, 30 (1997) 8499-8504.
[6] Z. Zhong, S. Zheng, Y. Mi, High-pressure DSC study of thermal transitions of a poly(ethylene terephthalate)/carbon dioxide system, Polymer, 40 (1999) 3829-3834.
[7] K. Mizoguchi, T. Hirose, Y. Naito, Y. Kamiya, CO_2-induced crystallization of poly(ethylene terephthalate), Polymer, 28 (1987) 1298-1302.
[8] J.S. Chiou, J.W. Barlow, D.R. Paul, Polymer crystallization induced by sorption of CO_2 gas, Journal of Applied Polymer Science, 30 (1985) 3911-3924.
[9] S.M. Lambert, M.E. Paulaitis, Crystallization of poly(ethylene terephthalate) induced by carbon dioxide sorption at elevated pressures, The Journal of Supercritical Fluids, 4 (1991) 15-23.
[10] E. Beckman, R.S. Porter, Crystallization of bisphenol a polycarbonate induced by supercritical carbon dioxide, Journal of Polymer Science Part B: Polymer Physics, 25 (1987) 1511-1517.
[11] C.A. Kelly, K.L. Harrison, G.A. Leeke, M.J. Jenkins, Detection of melting point depression and crystallization of polycaprolactone (PCL) in $scCO_2$ by infrared spectroscopy, Polym J, 45 (2013) 188-192.
[12] E. Markočič, M. Škerget, Ž. Knez, Effect of Temperature and Pressure on the Behavior of Poly(ε-caprolactone) in the Presence of Supercritical Carbon Dioxide, Industrial & Engineering Chemistry Research, 52 (2013) 15594-15601.
[13] Y.-T. Shieh, H.-S. Yang, Morphological changes of polycaprolactone with high-pressure CO2 treatment, The Journal of Supercritical Fluids, 33 (2005) 183-192.
[14] Y.P. Handa, Z. Zhang, J. Roovers, Compressed-gas-induced crystallization in tert-butyl poly(ether ether ketone), Journal of Polymer Science Part B: Polymer Physics, 39 (2001) 1505-1512.
[15] Y.P. Handa, J. Roovers, F. Wang, Effect of Thermal Annealing and Supercritical Fluids on the Crystallization Behavior of Methyl-Substituted Poly(aryl ether ether ketone), Macromolecules, 27 (1994) 5511-5516.
[16] J.D. Schultze, I.A.D. Engelmann, M. Boehning, J. Springer, Influence of sorbed carbon dioxide on transition temperatures of poly(p-phenylene sulphide), Polymers for Advanced Technologies, 2 (1991) 123-126.
[17] S. Takahashi, E. Kiran, Development of ring-banded spherulitic morphologies and formation of radially oriented nano-pores in poly(3-hydroxybutyrate-co-3-hydroxyvalerate) during crystallization in CO_2, The Journal of Supercritical Fluids, 96 (2015) 359-368.
[18] R. Bhomia, V. Trivedi, J.C. Mitchell, N.J. Coleman, M.J. Snowden, Effect of Pressure on the Melting Point of Pluronics in Pressurized Carbon Dioxide, Industrial & Engineering Chemistry Research, 53 (2014) 10820-10825.

[19] H. Lin, B.D. Freeman, Materials selection guidelines for membranes that remove CO_2 from gas mixtures, Journal of Molecular Structure, 739 (2005) 57-74.
[20] H. Wang, J.K. Keum, A. Hiltner, E. Baer, B. Freeman, A. Rozanski, A. Galeski, Confined Crystallization of Polyethylene Oxide in Nanolayer Assemblies, Science, 323 (2009) 757-760.
[21] H. Lin, B.D. Freeman, Gas solubility, diffusivity and permeability in poly(ethylene oxide), Journal of Membrane Science, 239 (2004) 105-117.
[22] S.J. Metz, M.H.V. Mulder, M. Wessling, Gas-Permeation Properties of Poly(ethylene oxide) Poly(butylene terephthalate) Block Copolymers, Macromolecules, 37 (2004) 4590-4597.
[23] V.I. Bondar, B.D. Freeman, I. Pinnau, Gas sorption and characterization of poly(ether-b-amide) segmented block copolymers, Journal of Polymer Science Part B: Polymer Physics, 37 (1999) 2463-2475.
[24] M.M. Rahman, V. Filiz, M.M. Khan, B.N. Gacal, V. Abetz, Functionalization of POSS nanoparticles and fabrication of block copolymer nanocomposite membranes for CO_2 separation, Reactive and Functional Polymers, 86 (2015) 125-133.
[25] M.M. Rahman, V. Filiz, S. Shishatskiy, C. Abetz, P. Georgopanos, M.M. Khan, S. Neumann, V. Abetz, Influence of Poly(ethylene glycol) Segment Length on CO_2 Permeation and Stability of PolyActive Membranes and Their Nanocomposites with PEG POSS, ACS Applied Materials & Interfaces, 7 (2015) 12289-12298.
[26] S.J. Metz, N.F.A. van der Vegt, M.H.V. Mulder, M. Wessling, Thermodynamics of Water Vapor Sorption in Poly(ethylene oxide) Poly(butylene terephthalate) Block Copolymers, The Journal of Physical Chemistry B, 107 (2003) 13629-13635.
[27] M.M. Rahman, S. Shishatskiy, C. Abetz, P. Georgopanos, S. Neumann, M.M. Khan, V. Filiz, V. Abetz, Influence of Temperature upon Properties of Tailor-Made PEBAX® MH 1657 Nanocomposite Membranes for Post-Combustion CO_2 Capture, Journal of Membrane Science, 469 (2014) 344-354.
[28] M.M. Rahman, V. Filiz, S. Shishatskiy, C. Abetz, S. Neumann, S. Bolmer, M.M. Khan, V. Abetz, PEBAX® with PEG Functionalized POSS as Nanocomposite Membranes for CO_2 Separation, Journal of Membrane Science, 437 (2013) 286-297.
[29] Y. Sato, T. Takikawa, S. Takishima, H. Masuoka, Solubilities and diffusion coefficients of carbon dioxide in poly(vinyl acetate) and polystyrene, The Journal of Supercritical Fluids, 19 (2001) 187-198.
[30] R. Staudt, G. Sailer, M. Tomalla, J.U. Keller, A Note on Gravimetric Measurements of Gas-Adsorption Equilibria, Berichte der Bunsengesellschaft für physikalische Chemie, 97 (1993) 98-105.
[31] E. Aionicesei, M. Škerget, Ž. Knez, Measurement of CO_2 solubility and diffusivity in poly(l-lactide) and poly(d,l-lactide-co-glycolide) by magnetic suspension balance, The Journal of Supercritical Fluids, 47 (2008) 296-301.
[32] G. Soave, Equilibrium constants from a modified Redlich-Kwong equation of state, Chemical Engineering Science, 27 (1972) 1197-1203.
[33] H. Gamsjäger, J.W. Lorimer, P. Scharlin, D.G. Shaw, Glossary of terms related to solubility (IUPAC Recommendations 2008), Pure Appl. Chem., 80 (2008) 233-276.
[34] C. Leng, J.D. Kish, J. Kelley, M. Mach, J. Hiltner, Y. Zhang, Y. Liu, Temperature-Dependent Henry's Law Constants of Atmospheric Organics of Biogenic Origin, The Journal of Physical Chemistry A, 117 (2013) 10359-10367.
[35] F.T. Simon, J.M. Rutherfod, Crystallization and Melting Behavior of Polyethylene Oxide Copolymers, Journal of Applied Physics, 35 (1964) 82-86.

[36] K. Ghosal, B.D. Freeman, Gas separation using polymer membranes: an overview, Polymers for Advanced Technologies, 5 (1994) 673-697.
[37] M. Klopffer, H., B. Flaconneche, Transport Properties of Gases in Polymers: Bibliographic Review, Oil & Gas Science and Technology - Rev. IFP, 56 (2001) 223-244.
[38] L.-l. Dong, C.-f. Zhang, Y.-y. Zhang, Y.-x. Bai, J. Gu, Y.-p. Sun, M.-q. Chen, Improving CO2/N2 separation performance using nonionic surfactant Tween containing polymeric gel membranes, RSC Advances, 5 (2015) 4947-4957.
[39] G.K. Fleming, W.J. Koros, Dilation of polymers by sorption of carbon dioxide at elevated pressures. 1. Silicone rubber and unconditioned polycarbonate, Macromolecules, 19 (1986) 2285-2291.
[40] T.A. Barbari, R.M. Conforti, Recent theories of gas sorption in polymers, Polymers for Advanced Technologies, 5 (1994) 698-707.
[41] A.S. Michaels, R.B. Parker, Sorption and flow of gases in polyethylene, Journal of Polymer Science, 41 (1959) 53-71.
[42] A.S. Michaels, H.J. Bixler, Solubility of gases in polyethylene, Journal of Polymer Science, 50 (1961) 393-412.
[43] A.S. Michaels, H.J. Bixler, Flow of gases through polyethylene, Journal of Polymer Science, 50 (1961) 413-439.
[44] J.D. Hoffman, J.J. Weeks, Melting Process and the Equilibrium Melting Temperature of Polychlorotrifluoroethylene, J. Res. Bur. Stand., 66A (1962) 13 - 28.
[45] P.J. Flory, Phase Equilibria in Polymer Systems, in: Principles of Polymer Chemistry, Cornell University Press, Ithaca, Newyork, USA, 1953, pp. 568-571.
[46] L. Mandelkern, R.G. Alamo, Thermodynamic Quantities Governing Melting, in: J. Mark (Ed.) Physical Properties of Polymers Handbook, Springer New York, 2007, pp. 165-186.
[47] R. Schulze, M.M.L. Arras, C. Helbing, S. Hölzer, U.S. Schubert, T.F. Keller, K.D. Jandt, How the Calorimetric Properties of a Crystalline Copolymer Correlate to Its Surface Nanostructures, Macromolecules, 47 (2014) 1705-1714.
[48] K. Fischer, M. Wilken, J. Gmehling, The effect of gas pressure on the melting behavior of compounds, Fluid Phase Equilibria, 210 (2003) 199-214.
[49] E. Weidner, V. Wiesmet, Ž. Knez, M. Škerget, Phase equilibrium (solid-liquid-gas) in polyethyleneglycol-carbon dioxide systems, The Journal of Supercritical Fluids, 10 (1997) 139-147.
[50] K.-H. Illers, Heat of fusion and specific volume of poly(ethylene terephthalate) and poly(butylene terephthalate), Colloid and Polymer Science, 258 (1980) 117-124.

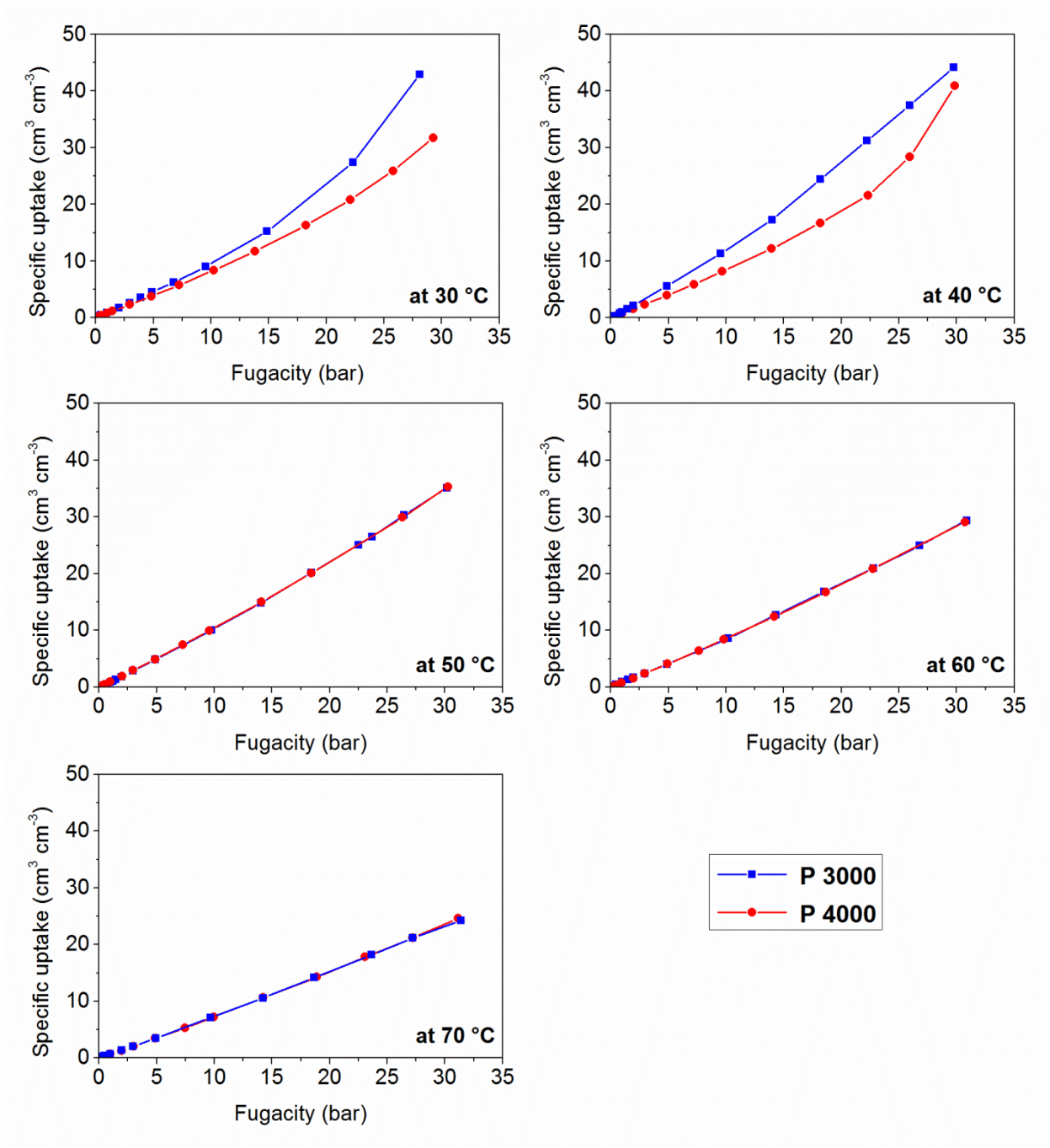

Figure 1: Specific CO_2 uptake of P 3000 and P 4000 vs fugacity at different temperatures.

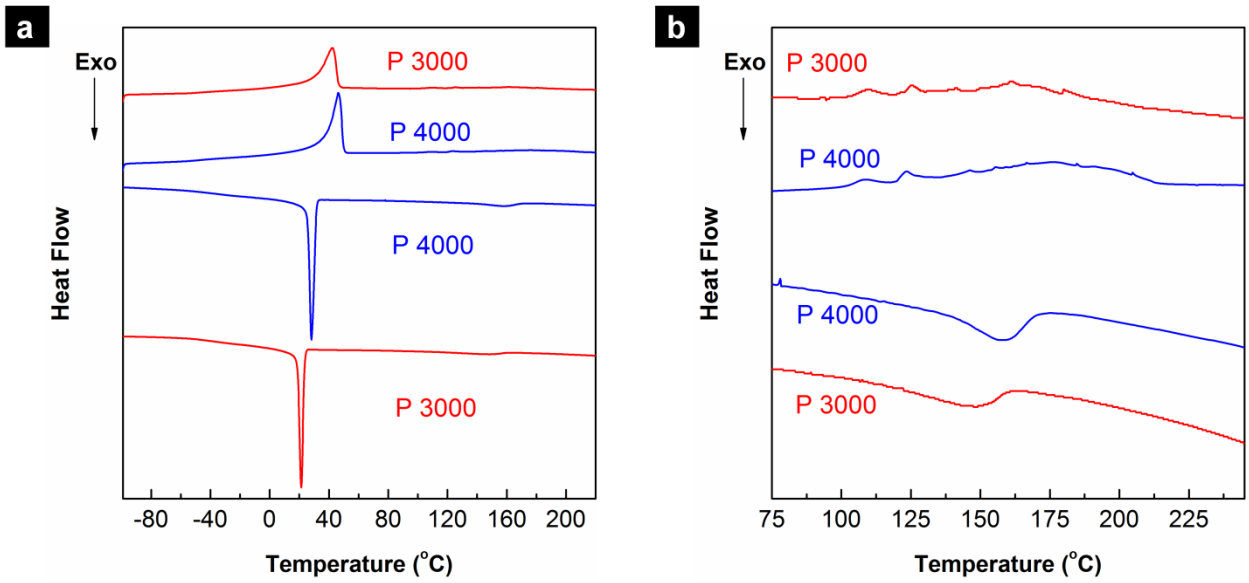

Figure 2: Differential scanning calorimetry traces for: a) two grades of PolyActive™ and b) PBT block of two grades of PolyActive™.

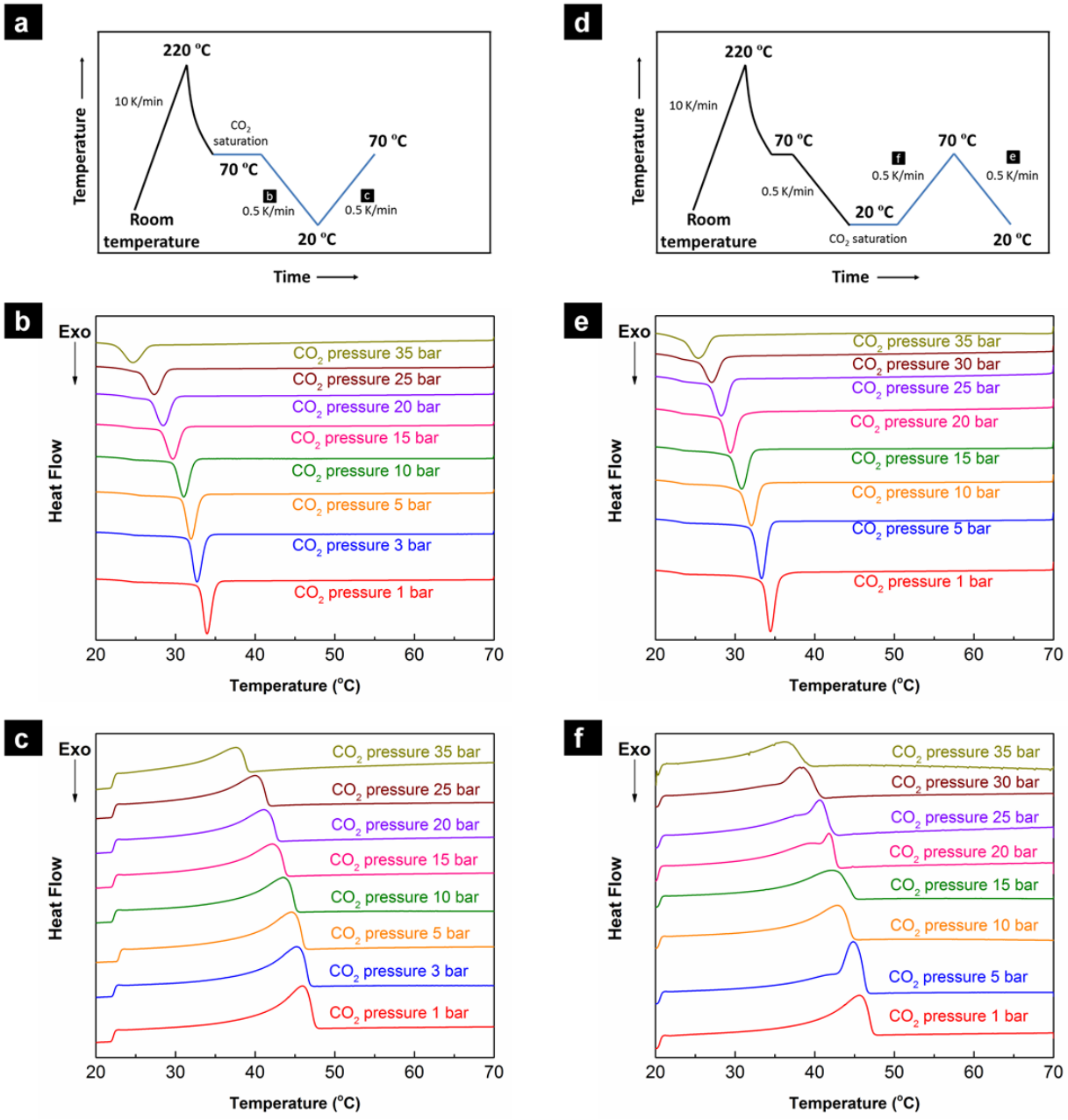

Figure 3: High pressure DSC traces of P 4000 for different CO_2 saturation pressures.

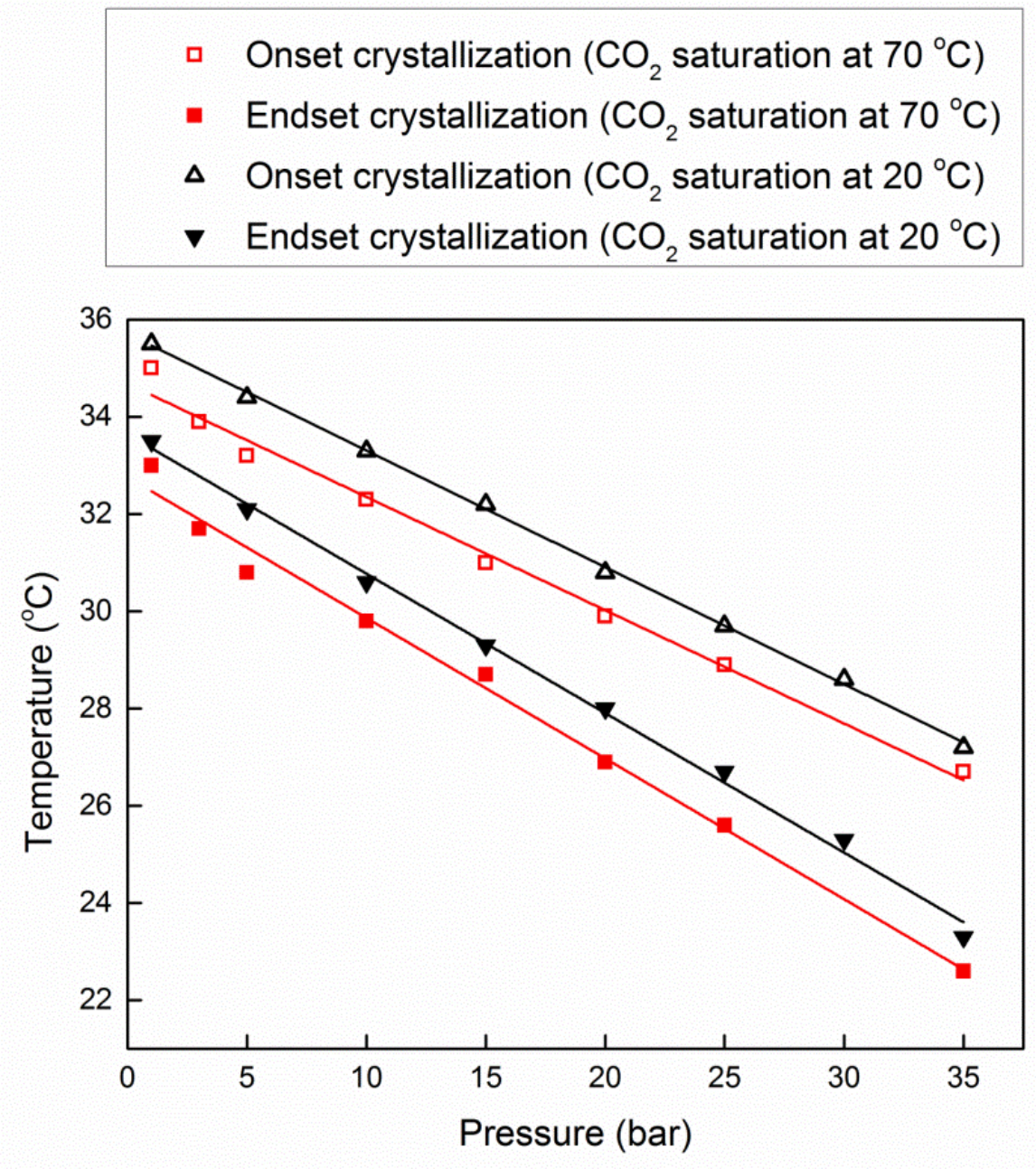

Figure 4: Comparison of onset and endset temperatures of crystallization of PEG block of P 4000 using different temperature protocols.

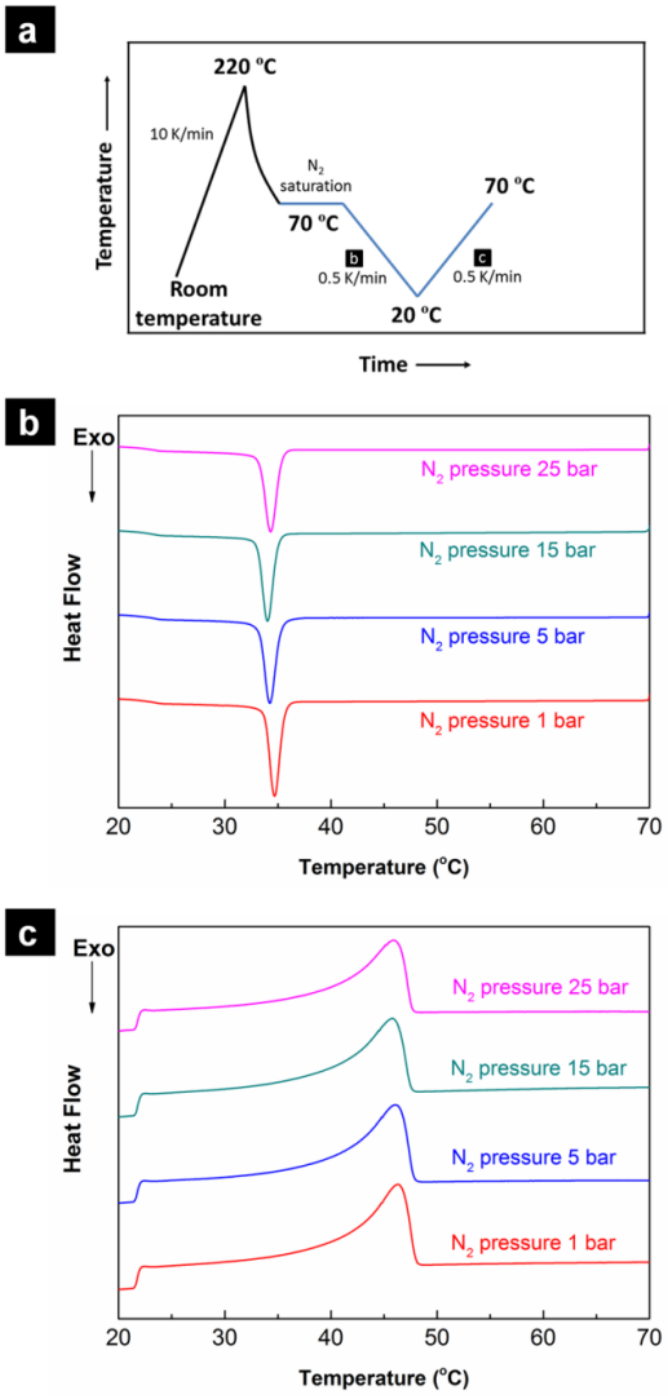

Figure 5: High pressure DSC traces of P 4000 for different N_2 saturation pressures.

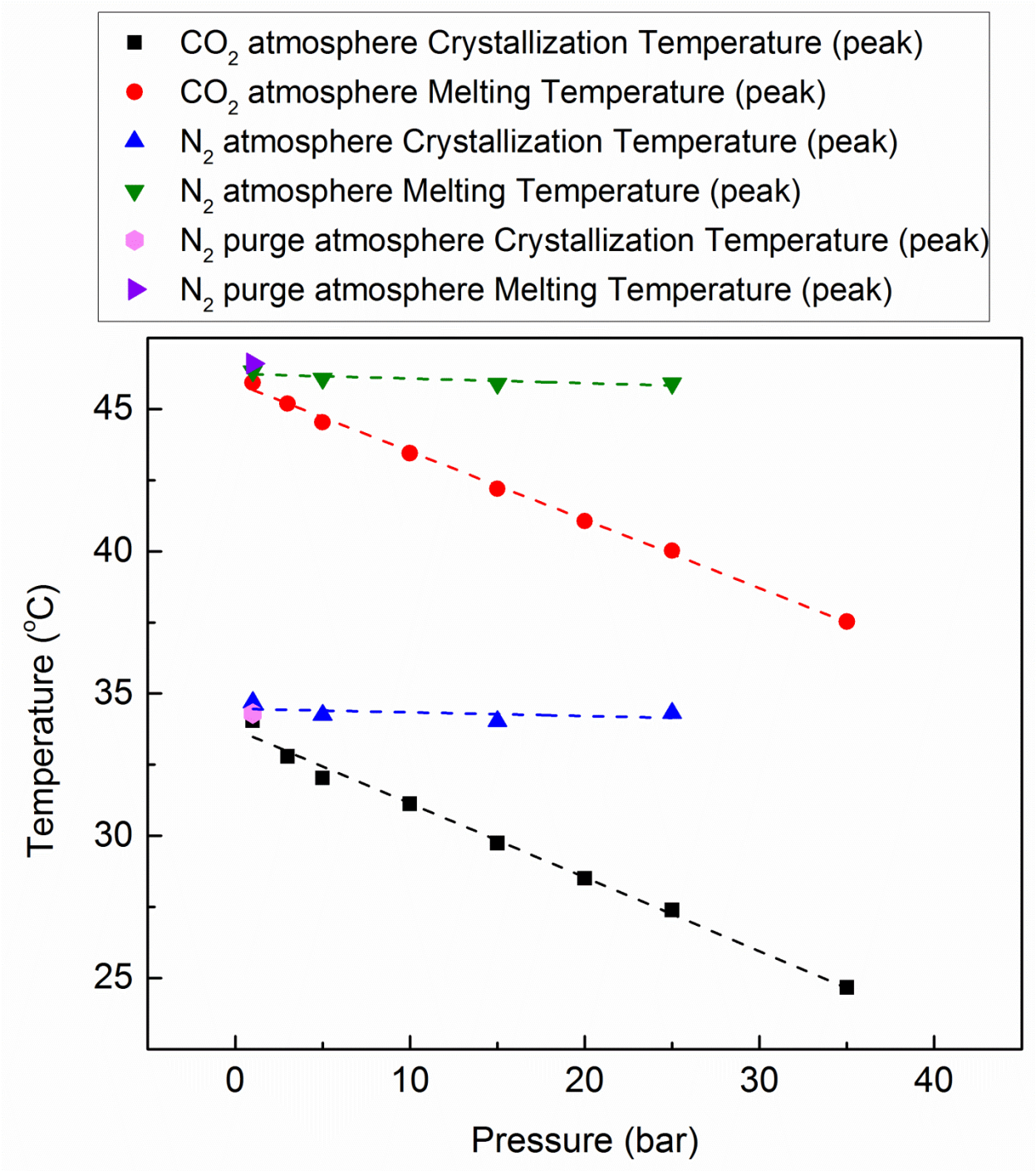

Figure 6: Melting and crystallization temperatures of PEG block of P 4000 determined in CO_2 and N_2 atmospheres.

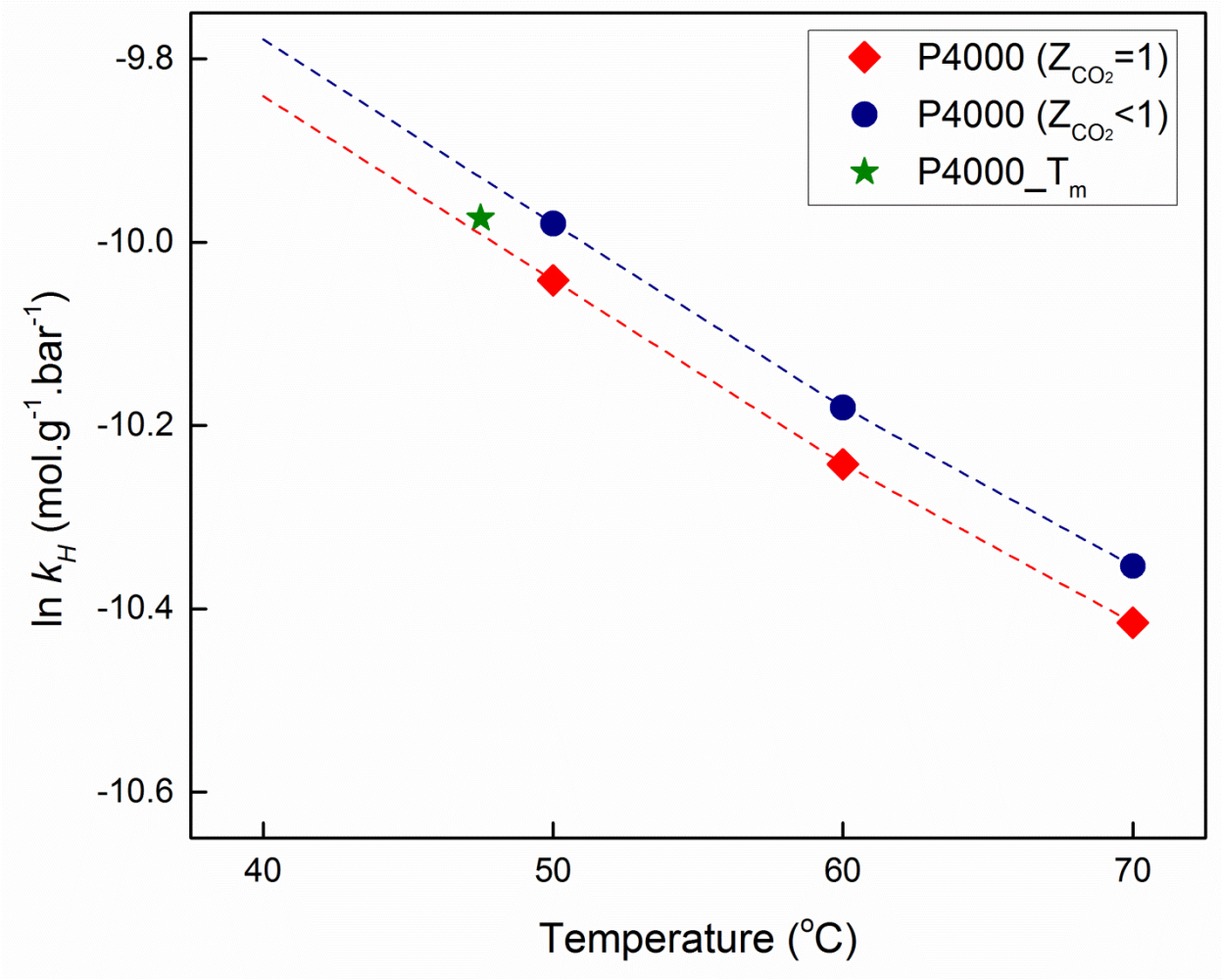

Figure 7: Comparison of Henry's law constant obtained from sorption balance and equation 11.

Table 1: Henry's law constant (k_H) and molar heat of CO_2 sorption (ΔHs) in P 3000 and P 4000 for ideal (i.e. compressibility factor of CO_2, $Z_{CO_2} = 1$) and real ($Z_{CO_2} < 1$) CO_2 gas behavior.

	Temperature [°C]	k_H x 10^{-5} [mol g^{-1} bar^{-1}]	ΔHs [kJ/mol]
P3000 (for $Z_{CO_2}<1$)	40 50 60 70	5.4 4.3 3.5 2.9	-18
P3000 (for $Z_{CO_2}=1$)	40 50 60 70	4.7 3.8 3.2 2.6	-17
P4000 (for $Z_{CO_2}<1$)	50 60 70	4.3 3.6 2.9	-17
P4000 (for $Z_{CO_2}=1$)	50 60 70	3.8 3.2 2.7	-16

Graphical abstract:

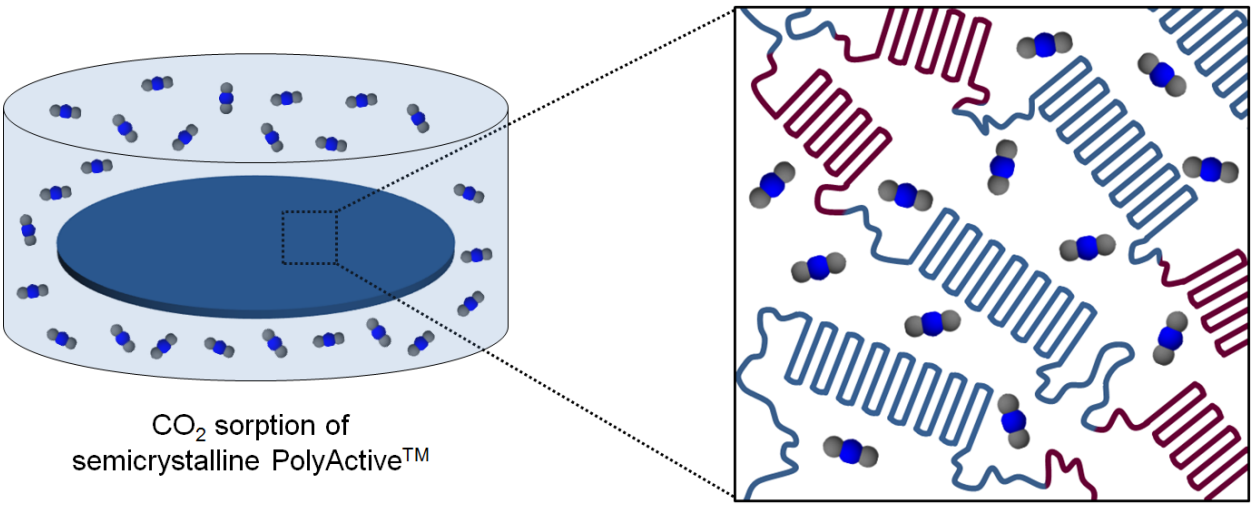

Supporting information

A thermodynamic study of CO_2 sorption and thermal transition of PolyActive™ under elevated pressure

Md. Mushfequr Rahman[a], Jelena Lillepärg[a], Silvio Neumann[a], Sergey Shishatskiy[a], Volker Abetz[a,b]*

[a]Helmholtz-Zentrum Geesthacht, Institute of Polymer Research, Max-Planck-Straße 1, 21502 Geesthacht, Germany

[b]University of Hamburg, Institute of Physical Chemistry, Grindelallee 117, 20146 Hamburg, Germany

*Corresponding Author. Email: volker.abetz@hzg.de

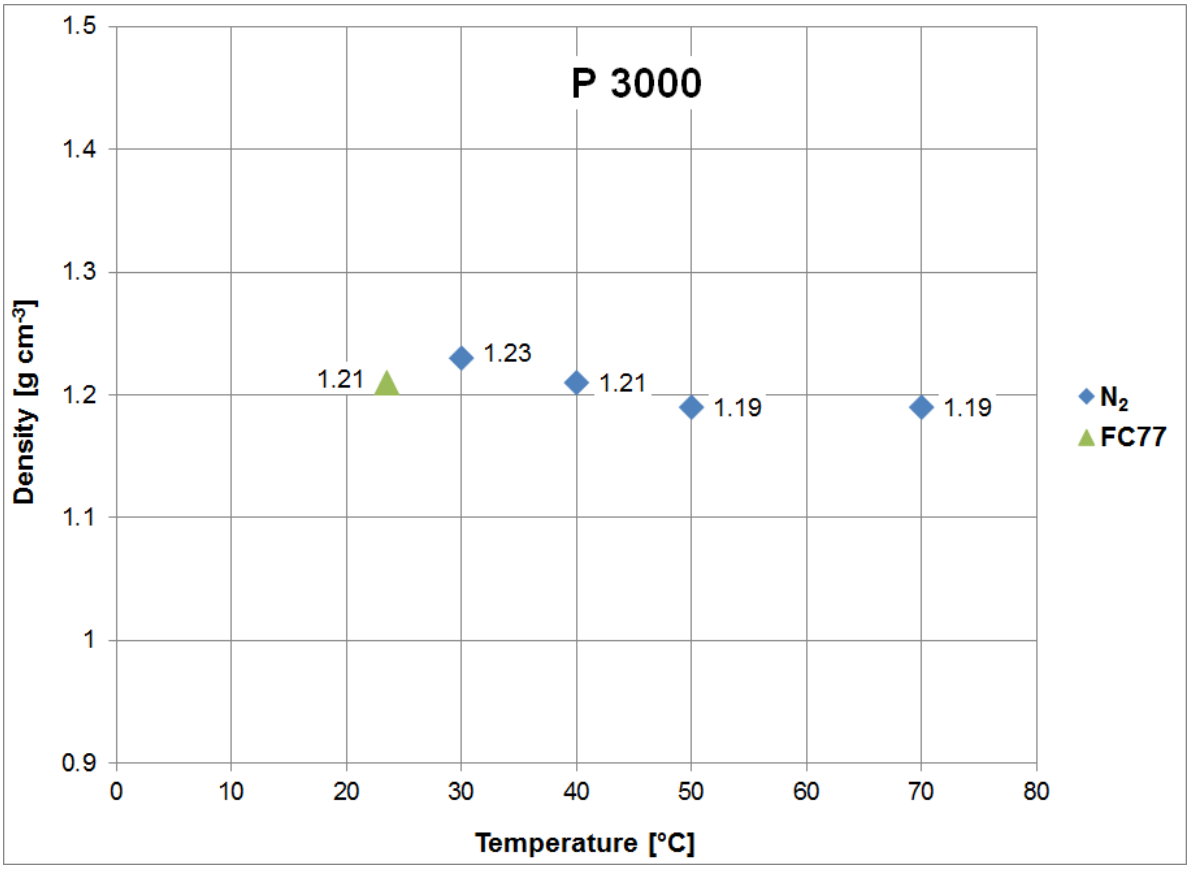

S 1: Density of P 3000 determined using magnetic suspension balance and Archimedes method.

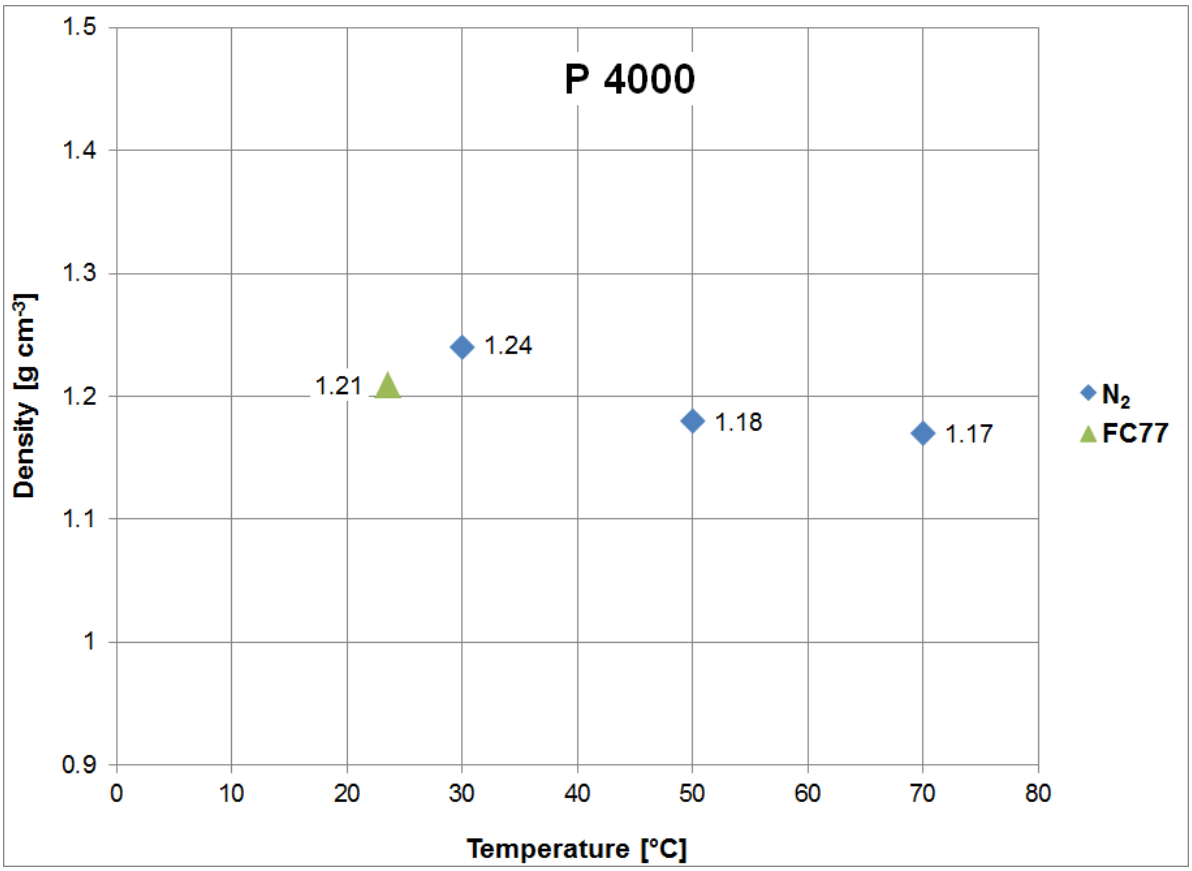

S 2: Density of P 4000 determined using magnetic suspension balance and Archimedes method.

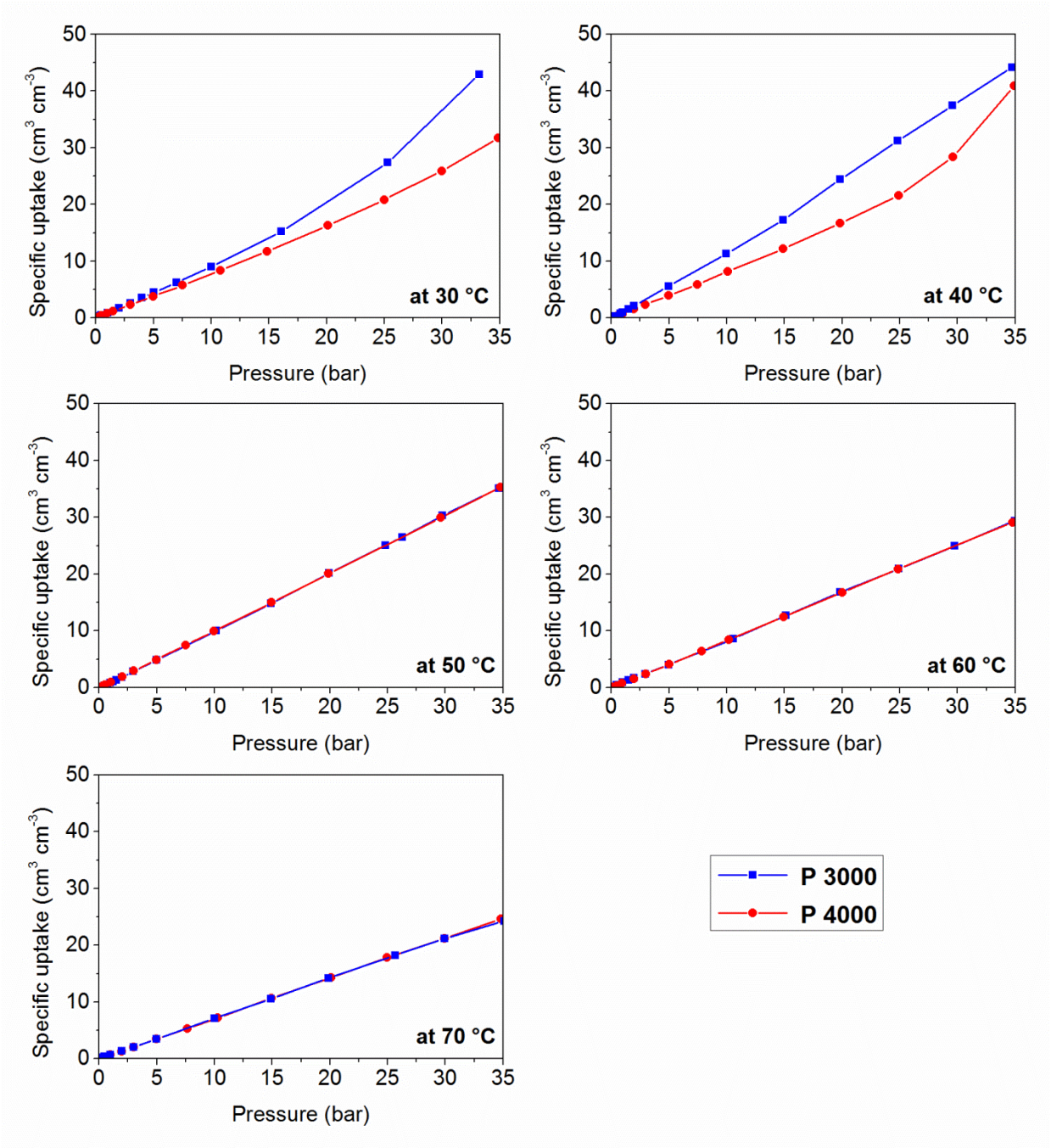

S 3: Specific CO_2 uptake of P 3000 and P 4000 vs Pressure at different temperatures.

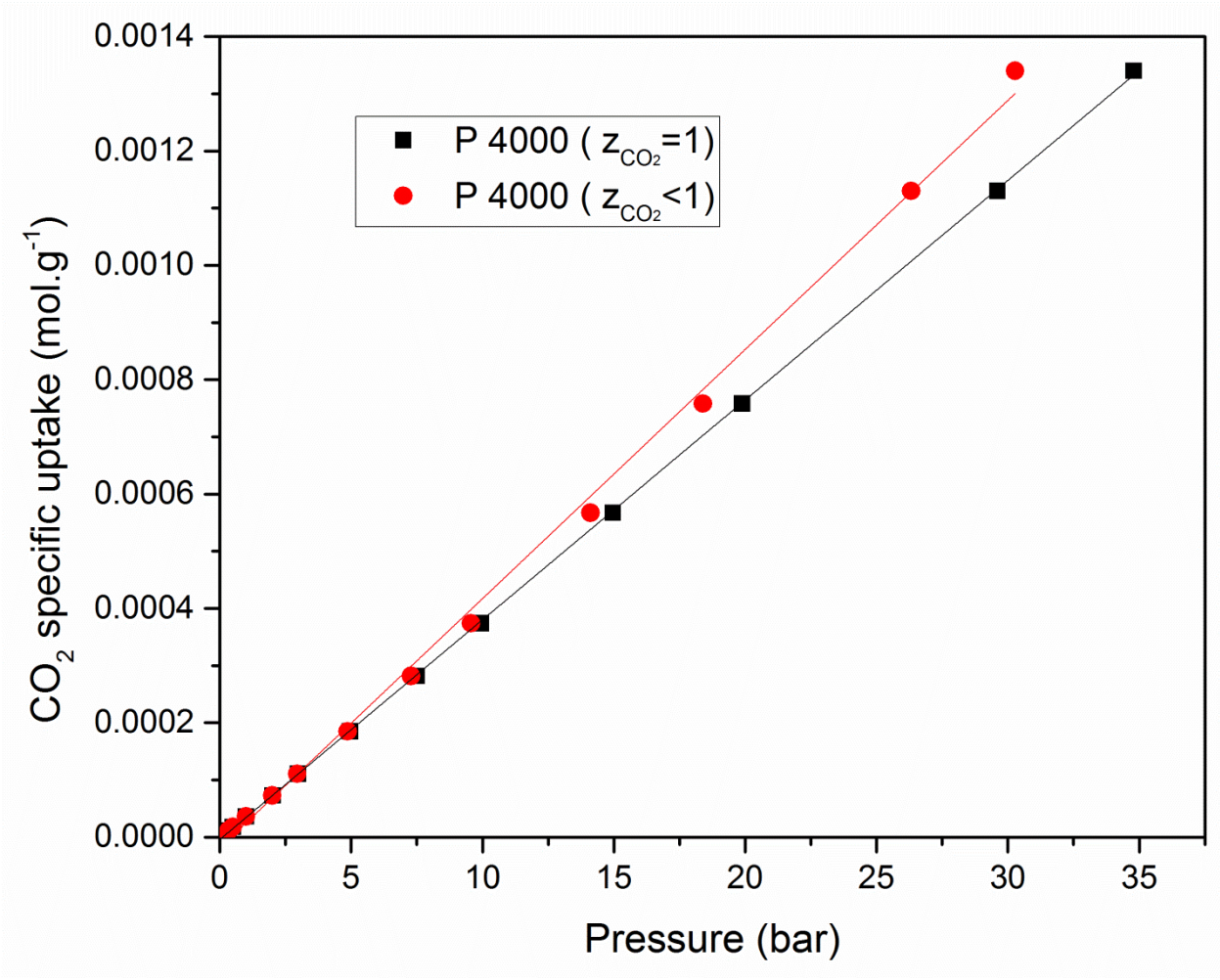

S 4: Linear fit of specific CO_2 uptake of P 4000 vs Pressure for ideal gas behavior of CO_2 ($Z_{CO_2} = 1$) and real gas behavior of CO_2 ($Z_{CO_2} < 1$).

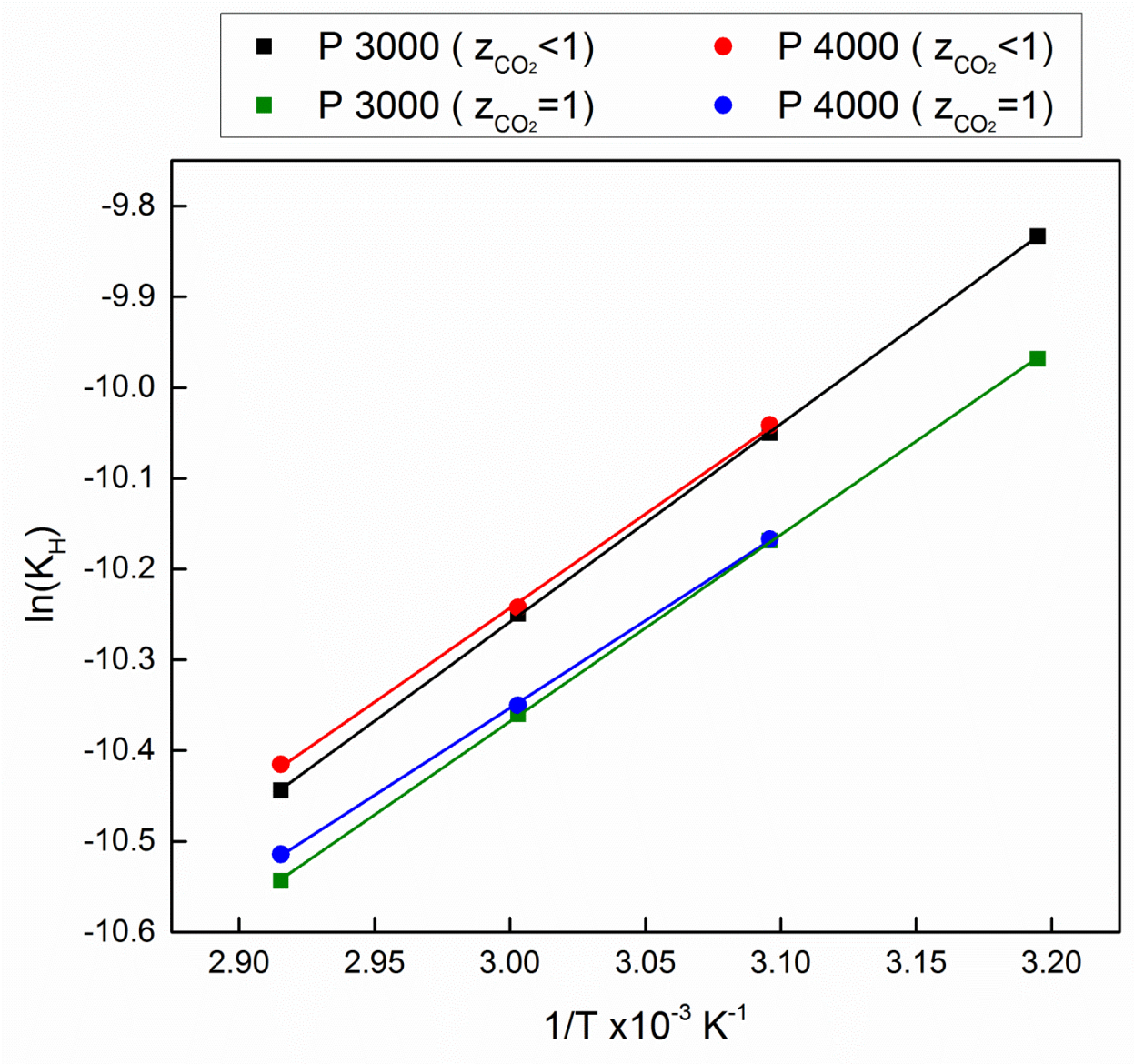

S 5: Plot of ln(K_H) vs 1/T of P 3000 and P 4000 for ideal gas behavior of CO_2 (Z_{CO_2} = 1) and real gas behavior of CO_2 (Z_{CO_2} < 1).

S 6: Melting and crystallization of the two blocks of PolyActive™ polymers.

	Onset (ºC)	Peak (ºC)	Endset (ºC)
P3000 PEG melting	32	41	45
P4000 PEG melting	40	46	50
P3000 PBT melting	105	-	205
P4000 PBT melting	105	-	205
P3000 PEG crystallization	23	21	18
P4000 PEG crystallization	30	28	25
P3000 PBT crystallization	160	149	108
P4000 PBT crystallization	170	160	132

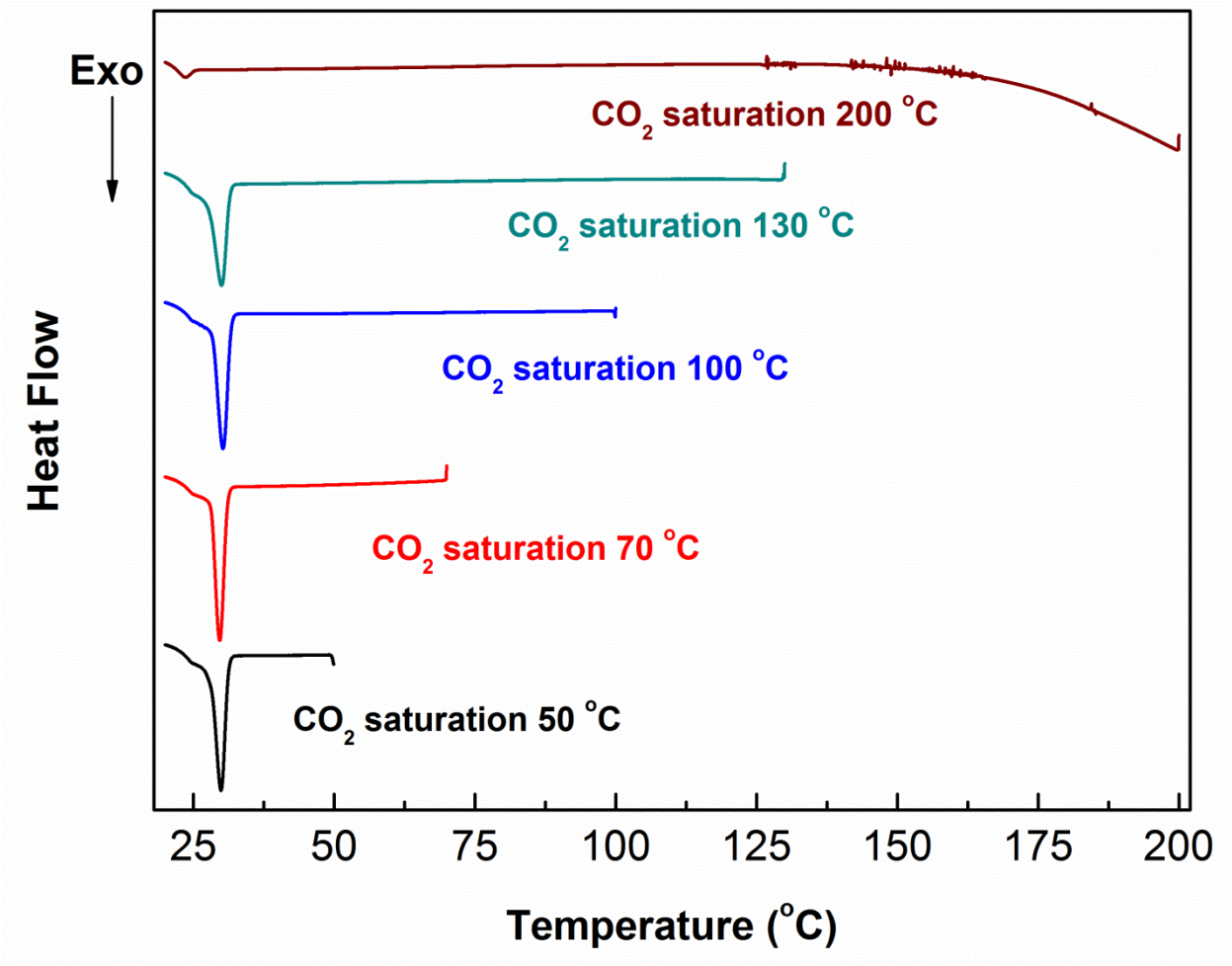

S 7: Crystallization of PEG block of P 4000 after 15 bar CO_2 saturation at different temperatures.

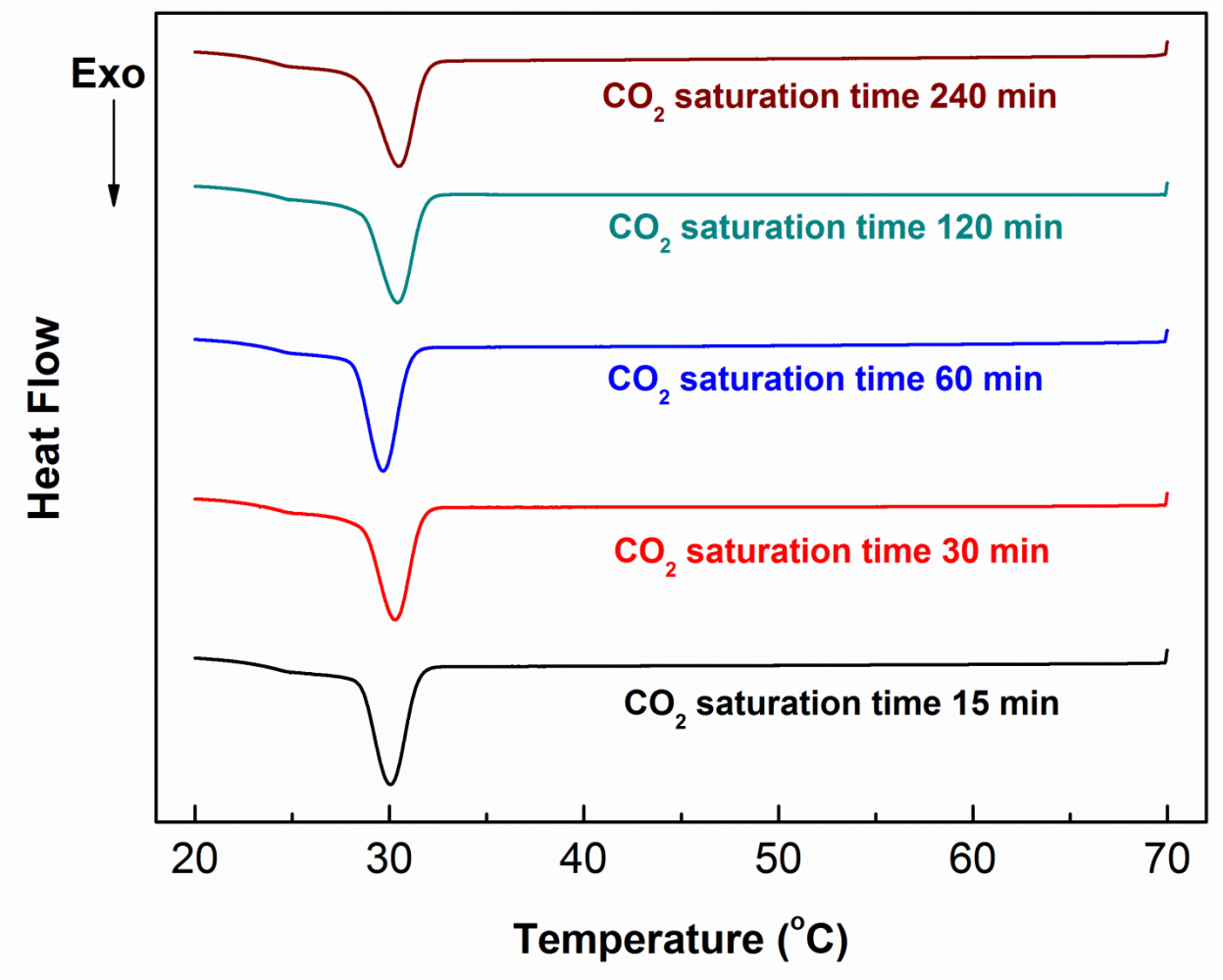

S 8: Crystallization of PEG block of P 4000 after 15 bar CO_2 saturation for different saturation times.

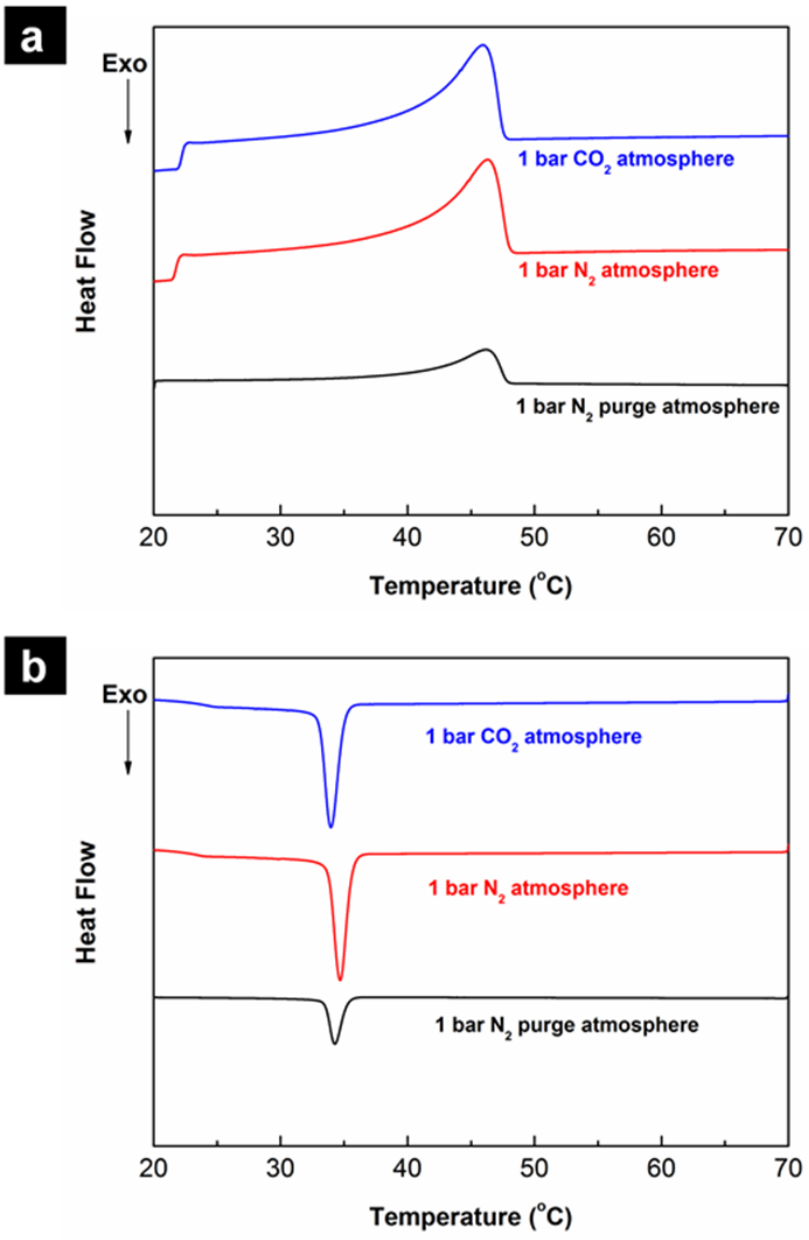

S9: Comparison of the thermal transitions of PEG block of P4000 at 1 bar N_2 and CO_2 atmosphere (high pressure DSC 1) and 1 bar N_2 purge atmosphere (DSC 1 (Star System)): a) second heating trace b) second cooling trace.

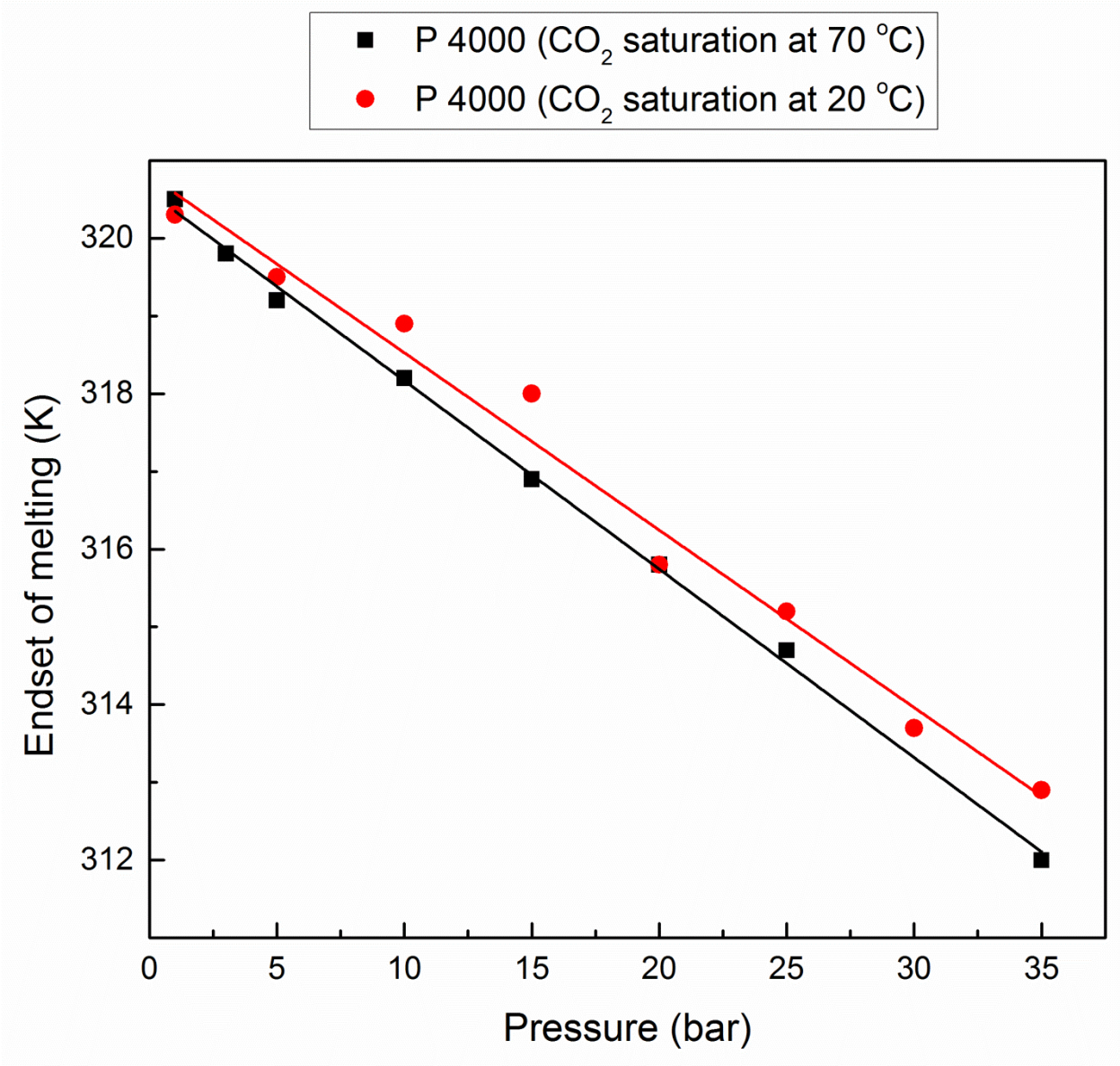

S10: Comparison of endset temperatures of melting of PEG block of P 4000 determined using different temperature protocols.